Characterization of TRPA1 from disease vector mosquitoes

Li, Tianbang

Doctor of Philosophy

Department of Physiological Sciences
School of Life Science
SOKENDAI (The Graduate University for Advanced Studies)

Doctoral Thesis

Characterization of TRPA1 from disease vector mosquitoes

Li, Tianbang

Supervisor:
Professor Makoto Tominaga

SOKENDAI (The Graduate University for Advanced Studies)
School of Life Science
Department of Physiological Sciences
2018

Word Count: 11181

ACKNOWLEDGEMENTS

I would like to thank the people who gave me supports in my project both academically and practically. First and foremost, I would like to acknowledge my supervisor Professor Makoto Tominaga for his supervision and efforts in all aspects of my work. I would also like to thank Dr. Shigeru Saito and Ms. Claire Saito for their day-to-day mentorship and inspiring advice throughout my study. I also gratefully acknowledge the other members in Tominaga's lab for their encouragement and support. I would like to extend my thanks to Professor Hirotaka Kanuka and Dr. Kayoko Yamaji (Jikei University School of Medicine) for their generous gift of experimental animal samples. Finally, I appreciate Professor Paul Garrity (Brandeis University) for providing me plasmid vectors which are necessary for this project.

Abstract

Mosquitoes have long been recognized as the primary vectors for transmission of malaria and other epidemic diseases in tropical and subtropical regions. The transient receptor potential channel, subfamily A, member 1 (TRPA1) channel of mosquitoes plays an important role in nociception. However, the physiological characteristics of mosquito TRPA1 have not been systematically studied. Here, TRPA1 from *Anopheles gambiae* (Ag), *Anopheles stephensi* (As), *Aedes aegypti* (Aa) and *Culex pipiens pallens* (Cp) were investigated. The responses of mosquito TRPA1s to heat or chemical stimuli were examined with calcium-imaging and whole-cell patch-clamp methods. Multiple TRPA1 channels have been cloned from disease vector mosquitoes, and several TRPA1 variants were identified. Fourteen amino acids were shown to be added at the N-terminus of TRPA1B, a modification that profoundly affected channel activity. The rates of heat ramps were strictly controlled because it was reported that the density of heat-evoked current was increased with them. While the rates did not affect temperature threshold for activation. Mosquito TRPA1 thermosensitivity was found to vary, and CpTRPA1 was found to have a lower temperature threshold for heat-evoked activation. Chemosensitivity of TRPA1 channels revealed differences not only between variants but also among orthologues. Finally, we discovered 3 novel mosquito TRPA1 agonists. Better understanding of the functional properties of mosquito TRPA1 may permit the design of improved control methods for mosquito-borne diseases.

Contents

List of figures

List of abbreviations

2-BEA- 2-(2-Butoxyethoxy) ethyl acetate

Aa- *Aedes egypti*

Ag- *Anopheles gambiae*

AITC- Allyl isothiocyanate

As- *Anopheles stephensi*

Cp- *Culex pipiens pallens*

DMSO- Dimethyl sulfoxide

HEK- Human embryonic kidney

Hs- Hymenoptera-specific

Mya- Million years ago

NUP- Nested Universal Primer

RACE- Rapid Amplification of cDNA Ends

TRPA1- Transient receptor potential ankyrin 1

UPM- Universal Primer A Mix

UTR- Untranslated region

CHAPTER 1

Introduction

1.1 Background

1.1.1 Disease vector mosquitoes investigated in this project

It is safe to state that mosquitoes are one of the most disliked insects in the environment. These tiny insects often show up near human residences at dusk. They often buzz around people's ears and disturb sleeping while seeking blood meals. Mosquitoes suck peripheral blood from animals (and humans), causing intense itching and, in some cases, spreading serious diseases.

These annoying tiny insects are among the deadliest animals in the world. Mosquitoes bite humans effectively by piercing their sophisticated proboscis under the skin into a blood vessel. With the proboscis, they also exude chemicals such as histamine to facilitate blood flow and leave itchy welts afterwards. Sometimes, they leave behind saliva that contains viruses or parasites that can cause diseases. For example, *Anopheles* mosquitoes are well known as the host species that spread malaria. From 200 to 300 million people are infected every year. Moreover, around 445,000 people died from malarial infection in 2016 (WHO, 2017). The most vulnerable people are children and pregnant women. Continued global warming may spread the range of these insects, promoting diseases in developing countries.

Anopheles gambiae is one of the most efficient malaria vectors known. It inhabits sub-Saharan Africa and is investigated in the present project. Although *Anopheles gambiae* includes many morphologically identical subgroups, *Anopheles stephensi*, a primary malaria vector in India, is not generally included in *Anopheles gambiae* complexes (Dash et al., 2007). Due to its importance, it is meaningful to include this mosquito species in this research as well.

In 2016, the summer Olympic Games held in Rio de Janeiro were seriously threatened by Zika fever. This disease is mainly spread via the bite of *Aedes* mosquitoes. Yellow fever is spread via *Aedes aegypti;* it defeated Napoleon's army in the jungles of Haiti. As one member

of the 3 most notorious genera of mosquitoes, *Aedes aegypti* inhabits an enormous territory in tropical and sub-tropical regions of the world and it deserves to be included in this mosquito study.

House mosquitoes are also widely distributed in the world except in frigid and desert zones. Their genus name is *Culex* and *Culex* mosquitoes are famous for spreading Japanese encephalitis virus, which was prevalent in Japan in earlier years. This disease is still epidemic in some places of mainland China. In Japan, there is concern that this vector might return. In Japan, the dominant *Culex* species is *Culex pipiens*. There are several subspecies of *Culex pipiens* inhabiting the Japanese archipelago, such as *Culex pipiens pallens, Culex pipiens molestus, Culex pipiens quinquefasciatus* and *Culex pipiens vagans. Culex pipiens pallens* originated in Nara prefecture and is the sole temperate mosquito species investigated in this project.

1.1.2 The host-seeking behavior of female mosquitoes depends on several sensory modalities

Carbohydrates constitute the primary energy source for mosquito activity in natural environments. Mosquito carbohydrate intake is mainly from nectars and the juices of ripe or rotten fruit. Only female mosquitoes possess a strong innate drive to find blood meals, which provide a protein source for egg development. However, non-blood feeding oviposition was reported in at least 15 mosquito groups (Clements et al., 1992). They can utilize the reserved energy for developing eggs for the first spawning after eclosion.

Female mosquitoes sense the presence of potential host animals by detecting carbon dioxide exhaled by animals, water vapor as well as skin odorants contained in sweat. They also sense warm temperatures to detect the presence of endotherms (van Breugel et al., 2015;

Carde, 2015). The attraction of mosquitoes toward potential hosts is initiated by detecting carbon dioxide emitted from vertebrates through exhaled breath and skin (Omondi et al., 2015). The fluctuation of carbon dioxide concentrations occurring 10 meters away from a potential host can trigger a strong attractive response, permitting mosquitoes to track the source of the carbon dioxide plume using optomotor anemotaxis (Kennedy, 1940). Meanwhile, the fluctuation of carbon dioxide reduces the threshold of mosquitoes for responding to skin odorants (Dekker et al., 2005). This facilitates a close approach to the host. The host-seeking activity of mosquitoes is positively correlated with the ratio of carbon dioxide and odorant concentrations (Eiras and Jepson, 1991).

Within a distance of 1 to 2 meters, skin odorants play a crucial role for mosquitoes to locate a host (Lacey et al., 2014). Heat and humidity are the last checkpoints for guiding the landing of mosquitoes. The antennal sensilla coeloconica of mosquitoes contains thermoreceptors for sensing both cold and warmth (Davis and Sokolove, 1975). In a recent study, researchers discovered that transient receptor potential ankyrin 1 (TRPA1) protein is required for specialized host-selective thermotaxis in mosquitoes. Mutant mosquitoes without the *TrpA1* gene showed reduced avoidance of high temperatures (Corfas and Vosshall, 2015), suggesting that TRPA1 is not necessary for warm temperature-induced attraction in mosquitoes. Moreover, *TrpA1* expression was found in the distal antennal neurons of mosquitoes. When this gene was expressed in a heterologous system, it responded to heat stimuli up to 37^{o}C. It is possible that the expression of *TrpA1* in small coeloconic sensilla is responsible for the peripheral thermal responses (Wang et al., 2009).

1.1.3 TRPA1 channel: a candidate for involvement in mosquito avoidance behaviors

Transient receptor potential (TRP) ion channels play important roles in sensation of thermal and chemical stimuli (Caterina et al., 1997; Tominaga et al., 1998; Story et al., 2003). TRP channels were initially cloned from *Drosophila melanogaster* (Montell and Rubin., 1989). These nonselective cation channels are located on the plasma membrane of cells. TRP channels can be divided into seven subfamilies, including TRPV (Vanilloid), TRPA (Ankyrin), TRPM (Melastatin), TRPC (Canonical), TRPN (NompC), TRPP (Polycystic) and TRPML (Mucolipin). TRP channels form tetramers and each subunit consists of six transmembrane domains and cytoplasmic N- and C-termini. The channel pore is located between the fifth and the sixth transmembrane domains. TRPA1 is the only member of the TRPA subfamily in mammals, and one distinguishing characteristic of TRPA1 is the extensive repeating of ankyrin domains in the amino-terminus. TRPA1 is mainly expressed in sensory neurons such as dorsal root ganglia and trigeminal ganglion neurons (Story et al., 2003). Human TRPA1 structure has been determined using a single-particle analysis with a cryo-electron microscope at a high resolution (~ 4 Å) in the presence of agonist or antagonist (Paulsen et al., 2015).

TRPA1 is required for thermal sensation. Mouse TRPA1 is reportedly activated by low temperatures (Story et al., 2003). TRPA1 plays a role in high temperature sensation in many non-mammalian species, including mosquitoes (Hamada et al., 2008; Saito et al., 2012; Kang et al., 2012). In insects, TRPA1 is required for avoiding noxious heat. In *Drosophila*, knock down of *TrpA1* significantly compromises the thermotactic behavior of the third instar larvae (Rosenzweig et al., 2005). Analogously, *Aedes aegypti* TRPA1 was found necessary to distinguish the difference between a warm host (~37^{o}C) and a hot object (> 43^{o}C) (Corfas and Vosshall, 2015). *Drosophila* larvae exhibited a TRPA1-dependent nociceptive rolling behavior when they were subjected to a rapid temperature increase (Luo et al., 2016).

TRPA1 also serves as a chemical receptor. Electrophilic irritants and pungent substances such as allyl isothiocyanate (AITC) and cinnamaldehyde potently activate TRPA1 via covalent modification of critical cysteine residues located in the ankyrin repeat domain and nearby linker region (Hinman et al., 2006; Macpherson et al., 2007). In a behavioral assay of fruit flies, a dramatic inhibition of proboscis extension responses was observed when AITC was added to the sucrose solution. In contrast, loss-of-function mutants of *TrpA1* of *Drosophila* showed no reduction in proboscis extension responses when sucrose solution was mixed with AITC or other reactive electrophiles (Kang et al., 2010). Indeed, TRPA1 agonists were found to be promising repellents for specific animal species such as parasitic mites, mosquitoes and birds (Peng et al., 2015a; Inocente et al., 2018; Majikina et al., 2018).

1.1.4 The TRPA1 channel has been characterized in many animal species

Metazoan TRP channels have a very ancient origin. The TRPA subfamily was found in choanoflagellates (Cai, 2008). As expected, TRP channels are shared from simple microbes to mammals. TRPA1 functions as a polymodal nociceptive sensor for noxious cold (Viswanath et al., 2003) or hot (Neely et al., 2011; Zhong et al., 2012) temperatures, mechanical stress (Dunham et al., 2008) and irritant chemicals (Kang et al., 2010). Many researchers have characterized the function of TRPA channels from diverse animal species. TRPA subfamily members show very high diversity among arthropod species (Matsuura et al., 2009; Peng et al., 2015b). Such diversity may have resulted from the evolutionary plasticity of TRPA subfamily members through multiple gene-gain and -loss events (Kadowaki, 2015). Insects sense different temperature upon employing different TRP channels. In fruit flies, in addition to TRPA1, Painless and Pyrexia also play important roles in thermal nociception, although they are gated by different temperatures (Tracey et al., 2003; Lee et al., 2005). *Painless* and *pyrexia*

are basal *TrpAs* that diverged from a common ancestral *TrpA1* gene. However, they are not members of the modern *TrpA1* clade, and neither channel possesses adequate conserved electrophilic detection residues for chemical nociception (Kang et al., 2010).

Drosophila melanogaster's TRPA1 has multiple isoforms due to alternative splicing and at least 4 of them have been identified. The gene structures of these 4 variants differ not only within the 5' exon, which encodes the N-terminus but also among the 12th exon, which encodes a linker region between the ankyrin repeat domain and transmembrane domain (Zhong et al., 2012). *Drosophila melanogaster* TRPA1 splicing variants are expressed in different tissues and show distinct chemical and thermal sensitivities (Zhong et al., 2012; Kang et al., 2012; Luo et al., 2016). There are 2 splicing variants of murine *Trpa1*, i.e., *Trpa1a* and *Trpa1b*. TRPA1b loses 30 amino acids because one exon is skipped during translation. TRPA1b is insensitive to chemical stimuli, but it increases the response of TRPA1a to agonists by working as a chaperone (Zhou et al., 2013). In mosquitoes, TRPA1 variants were only investigated in *Anopheles gambiae*, and different N-termini of TRPA1 variants apparently possessed distinct thermosensitivities and chemosensitivities (Kang et al., 2012; Du et al., 2015). The question whether this phenomenon is consistent in other disease vector mosquitoes remains to be answered.

The function of the N-terminal ankyrin repeat domain has been a hotly contended topic in TRPA1 research. Through studies with channel chimeras, researchers deduced that the ankyrin repeat domain integrates diverse physiological signals to regulate the conformation of the channel for activation (Cordero-Morales et al., 2011). Another research group proposed that the N-terminus acts as a soft spring that directly connects to the channel pore (Zayats et al., 2013), which agrees with the high-resolution 3D reconstruction model of TRPA1 (Paulsen et al., 2015). However, some physiologists claim that the N-terminal ankyrin repeat

domain only modulates the responses to chemical or thermal stimuli, but is not necessary for activation (Survery et al., 2016). In the splicing variants of *Anopheles gambiae* TRPA1 so far identified, amino acid differences are observed only at the very end of the N-terminal domain (Kang et al., 2012). This region was not classified as a portable heat-sensitive module in a previous study (Cordero-Morales et al., 2011). A better understanding of the significance of this subtle region might unveil the mechanism by which TRPA1 is activated by temperature changes.

1.2 Plan of investigation

1.2.1 Research project questions and objectives

The African malaria mosquito (*Anopheles gambiae*) is the pre-eminent mosquito model for analyzing the efficiency and specificity of repellents. The yellow fever mosquito (*Aedes aegypti*) is another promising model for carrying out behavioral analysis. Both mosquito species are well-studied and their whole genomes have been sequenced. In a genome-wide, multigene phylogenetic analysis, the relationships among a number of disease vector mosquito species have been revealed. *Anopheles gambiae* and *Aedes aegypti* evolved separately from a common ancestor 147.6 million years ago (mya) (Kamali et al., 2014). Consequently, these species vary in a number of ways, including physiological characteristics, suggesting that these 2 species show different responses to mosquito repellents. In addition, understanding the differences observed in different mosquitos is inadequate because splicing variants of mosquito TRPA1 have not been systematically compared among different species. Therefore, my project includes *Anopheles stephensi* (diverged 30.4 mya from *Anopheles gambiae*) and *Culex pipiens* (diverged 56.9 mya from *Aedes aegypti*) as indispensable reference species to unveil how these plastic and dynamic TRPA1 channels have changed

through the evolutionary processes. Taken together, characterization of TRPA1s from disease vector mosquitoes could be useful in determining which TRPA1 variant to recruit for a particular mosquito study.

1.2.2 Hypotheses and aims

In this study, splicing variants of *TrpA1* from 4 different mosquito species (*Anopheles gambiae, Anopheles stephensi, Aedes aegypti* and *Culex pipiens pallens*) will be identified. Then, they will be subcloned into expression vectors and channel properties will be examined using calcium-imaging and whole-cell patch-clamp methods. Channel properties will be compared among the 4 mosquito species regarding chemical and thermal responses. The results could show that there is a diversity of channel properties among splicing variants and also among species. I will also seek several novel agonists for TRPA1. Therefore, the results of the present study will supply important information for future behavioral studies using diverse mosquito species and will also be useful for development of novel mosquito repellents.

CHAPTER 2

Materials and Methods

2.1 Animals

Adult mosquito samples of wild-type *Anopheles stephensi*, wild-type *Aedes aegypti*, wild-type *Culex pipiens pallens* (Nara Prefecture) and pupa of wild-type *Aedes aegypti* were reared and provided by Professor Hirotaka Kanuka, Department of Tropical Medicine, Jikei University School of Medicine.

2.2 Molecular cloning of mosquito TrpA1

2.2.1 Sub-cloning of *Anopheles gambiae TrpA1*

Template plasmid DNA of *Anopheles gambiae TrpA1(A)* and *Anopheles gambiae TrpA1(B)* were kindly provided by Professor Paul Garrity of Brandeis University.

For amplification of *Anopheles gambiae TrpA1(A)*, the sequences of the forward and reverse primers were designed as follows: 5'-TTTGGATCCACCATGCCTACTCCGCTG-3' and 5'- TAAGCGGCCGCTCATTTGCCAATAGATTTG-3'.

For amplification of *Anopheles gambiae TrpA1(B)*, the sequences of the forward and reverse primers were designed as follows: 5'-TTAGGATCCACCATGTGGCGCAACTG-3' and 5'-TAAGCGGCCGCTCATTTGCCAATAGATTTG-3'.

2.2.2 RNA extraction

The mosquitoes were fixed in RNAlater solution (Ambion) to preserve the RNA for subsequent extraction. Total RNA was extracted from the homogenized whole bodies of mosquito samples using chloroform, 2-propanol and 75% ethanol in turn. Total RNA was finally eluted in RNAse free Milli-Q water and stored at -80^{o}C.

2.2.3 cDNA synthesis

The cDNAs of all 3 mosquito species were synthesized from total RNAs (up to 1 μg) using ReverTra Ace (TOYOBO). For *Anopheles stephensi* and *Aedes aegypti*, their cDNA was also synthesized from total RNA using SMARTScribe Reverse Transcriptase (Clontech).

2.2.4 5’ and 3’ Rapid Amplification of cDNA Ends (RACE)

Primers were designed for 5’ and 3’ RACE of *Anopheles stephensi*, *Aedes aegypti* and *Culex pipiens pallens* according to the genomic sequences of *Anopheles gambiae*, *Aedes aegypti* and *Culex pipiens quinquefasciatus*, respectively. In 5’ and 3’ RACE, Universal Primer A Mix (UPM), 5'–CTAATACGACTCACTATAGGGCAAGCAGTGGTATCAACGCAGAGT–3' and Nested Universal Primer A (NUP), 5'–AAGCAGTGGTATCAACGCAGAGT–3' were used (Clontech).

For *Anopheles stephensi*, 2 primers, 5’- GTGTACGGCCGAGTGCAGTG-3’ (for the first PCR) and 5’-CTCCCGCGTGCATCCCTTCG-3’ (for the second PCR) were used for 5’ RACE. 3’ RACE was carried out as above except the following 2 primers were used: 5’-TTCACTCGCATCTGCTGGACC-3’ (for the first PCR) and 5’-AAGCTGCTGCACAACTACATGG-3’ (for the second PCR).

For *Aedes aegypti*, 2 primers, 5’-GGTGAGAATATTGATGCGGTTCC-3’ (for the first PCR) and 5’-CGTCCTTTGCTATCCTTCACC-3’ (for the second PCR) were used for 5’ RACE. 3’ RACE was carried out as above except the following 2 primers were used: 5’-TTCACTCGCATCTGCTGGACC-3’ (for the first PCR) and 5’-AAGCTGCTGCACAACTACATGG-3’ (for the second PCR).

For *Culex pipiens pallens*, 2 primers, 5’-AGAAAGTCCATCTCGCCCAGCATC-3’ (for the first PCR) and 5’-CATGACGACGTAGAGACCAACCTG 3’ (for the second PCR) were used for 5’ RACE. 3’ RACE was carried out as above except the following 2 primers were used: 5’-GGAAAAGGGAACCTTCATCATCAACG-3’ (for the first PCR) and

5’- CGCAACGATGGAGAACAGACC-3’ (for the second PCR).

2.2.5 Nested PCR

Ordinary PCR can amplify uncharacterized primer binding sites when primer designs are based on the genomic sequence of closely related species. Hereby, nested PCR was employed involving 2 or 3 sets of primers to intentionally amplify a secondary or a tertiary target within the previous run product. This allows the second or the third nested primers to specifically amplify the intended product from the first round of PCR.

Based on the information read from Untranslated Regions (UTR), nested PCR primers were designed to clone mosquito *TrpA1* step by step.

For *Anopheles stephensi*, the sequences of the forward and reverse primers were as follows: 5’-TCAGTCGTTCATCAACAGCATC-3’ (A)/ 5’-CATCGAAGGTACAGCAGTAGCAG-3’ (B) and 5’-ACACACACGTACACGTACAAGCTC-3’ (for the first PCR); 5’-TCAGTCGTTCATCAACAGCATC-3’ (A)/ 5’-CCCAAACCCATCAAGTGCAC-3’ (B) and 5’-TAAGCGGCCGCGTGGCTCCGCTACAGTGC-3’ (for the second PCR); 5’-CTTGTGTCCTCTGAACGATGC-3’ (A) and 5’-TAAGCGGCCGCACAGTGCCATTCATTTTCC -3’ (for the third PCR).

For *Aedes aegypti*, the sequences of the forward and reverse primers were as follows: 5’-CAATCAGACGAAATCCACCACTAGCC-3’ (A)/ 5’-CTACTGTAAACCGTCCATCG-3’ (B) and 5’-CAAAATTCGTTGTCCTGCTG-3’ (for the first PCR); 5’-CTCGGATCCACCATGCCAACTCCGCTC-3’ (A)/ 5’-CTCGGATCCACCATGTTACCAATTATGATG-3’ (B) and 5’-TAAGCGGCCGCCTACTTGCTAATCGACTTG-3’ (for the second PCR).

For *Culex pipiens pallens*, the sequences of the forward and reverse primers were as follows: 5’-CAACCCCCTACGGAAGAATCGCTAC-3’ (A)/ 5’-GTCCACGGTAACCATCGTCCATATCAG-3’ (B) and 5’-TCTCTCGCATTACTTGCTCATGGACTTG-3’ (for the first PCR);

5’-CTTGGATCCACCATGCCAACTCCGCTG-3’ (A)/

5’-CTCGGATCCACCATGATTAACCGGAAATCAATC-3’ (B) and

5’-TAAGCGGCCGCTTACTTGCTCATGGACTTG-3’ (for the second PCR).

2.2.6 Synthesis of longer *Anopheles gambiae TrpA1(B)*

Due to the fact that live samples of *Anopheles gambiae* were unavailable, we had to synthesize *Anopheles gambiae TrpA1(B)* with 14 amino acids at the N-terminus (to be explained in section **3.1**). A longer *Anopheles gambiae TrpA1(B)*-pcDNA3.1(+) plasmid was synthesized with a HiFi DNA Assembly Cloning Kit (NEB). First, shorter *Anopheles gambiae TrpA1(B)* was digested with 2 restriction enzymes to generate 2 linearized fragments. Then, the coding sequence of 14 amino acids with appropriate flanking overhangs (purchased) was mixed with 2 enzyme-digested fragments of the linearized vector. Two sets of forward and reverse primers were designed: 5’-CTCTACGACATATGTGGCGCAACTGTGCAC-3’ and 5’-AATCGATAGCGCTCATGTCC-3’ (for amplifying elongated *TrpA1* N-terminus), plus 5’-TTAAGCTTGGTACCGAGCTCGGATCCACCATGTTATCTGTTGCTATGTATACACGCAAATCTCTACGACATATGTGGCGC-3’ and 5’-GCGCCACATATGTCGTAGAGATTTGCGTGTATACATAGCAACAGATAACATGGTGGATCCGAGCTCGGTACCAAGCTTAA-3’ (for amplifying the remainder of the vector sequence). Three overlapping sequences were assembled to generate a closed longer *Anopheles gambiae TrpA1(B)*- pcDNA3.1(+) plasmid.

2.2.7 Examination of PCR product or plasmid DNA containing target gene via sequencing

For direct sequencing of a PCR product, a DNA sample at 10 ng/μL was sufficient; for sequencing mosquito *TrpA1* within plasmids, a DNA sample concentration around 100 ng/μL or 200 ng/μL (for 2 different recipes) was sufficient.

Prepared DNA samples were mixed with diluted dye (Big Dye Terminator V 3.1 (SARSTEDT)) and the single primer (1 μM) to be amplified through thermal cycling. The generated product was spun down and preserved in formamide, which was heat treated at 95°C for 4 min and then subjected to sequencing with an ABI PRISM 3130xl Genetic Analyzer (Thermo Fisher Scientific).

The sequencing results were analyzed with DNADynamo (Blue Tractor Software, Ltd). To determine the intron-exon structure based on the genomic DNA sequence, sequencing data was further analyzed with Molecular Evolutionary Genetics Analysis (MEGA) (Pennsylvania State University).

2.2.8 Identification and nomenclature of mosquito *TrpA1* variants

The nomenclature of *TrpA1* variants differs among research groups. In this project, based on the nomenclature in a paper on mosquito *TrpA1* variants (Kang et al., 2012), a readily comprehensible way was designed to depict complicated mosquito *TrpA1* variants. According to exon location, the upstream exon was named “a”, and the downstream exon was named “b”. Upper case was used for locating variants in the N-terminus, lower case for locating in the middle part. N-terminal features are described in advance. In addition, when mosquito species names were combined with *TrpA1* to indicate a particular channel, *Anopheles gambiae*, *Anopheles stephensi*, *Aedes aegypti* and *Culex pipiens pallens* are abbreviated to Ag, As, Aa and Cp, respectively.

2.3 Cell culture

The human embryonic kidney cell line 293 (HEK293) is widely used in cell biology because the line is readily grown and the cells can be routinely transfected. HEK293 cells were used as hosts for TRPA1 expression for whole-cell patch-clamp recordings and calcium-imaging. HEK293 cells were cultured in Dulbecco's modified Eagle Medium (Wako) supplemented with 10% FBS (BioWest), penicillin-streptomycin (50 mg/mL and 50 units/mL, respectively, Gibco) and GlutaMAX (2 mM, Gibco). They were passaged at a density of approximately 2.5 x 10^5 or 5 x 10^5 cells per 35 x 10 mm FALCON dish 24 or 48 h before transfection. For transfection of HEK293 cells, 1 μg plasmid DNA in pcDNA3.1 (+) and 0.1 μg pGreen-Lantern 1 vector were transfected into HEK293 cells using Lipofectamine reagent and Plus reagent (Invitrogen) for subsequent whole-cell patch-clamp recording. In the case of transfection for calcium-imaging, 0.1 μg pCMV-DsRed vector was transfected instead of pGreen-Lantern 1 vector. All these components were dissolved in Opti-MEM I (1X, Gibco). After incubation for 3-4 h, HEK293 cells were reseeded on 12 mm cover slips (Matsunami) and further incubated at 33°C in 5% CO_2.

2.4 Calcium-imaging

A Fura-2 calcium-imaging method was employed to check the approximate responses of heterologously expressed TRPA1 channels to extracellular stimuli. Calcium-imaging was performed 18-30 h after transfection. The extracellular standard bath solution was the same as described in the Electrophysiology section below. Chemical and thermal stimuli were applied in the same manner as described in whole-cell patch-clamp recording. Cytosolic-free Ca^{2+} concentrations in HEK293 cells were measured by dual-wavelength fura-2 (Molecular Probes, Invitrogen Corp). Fura-2-acetoxymethyl ester (5 μM) was loaded 1 h before recording,

and it was excited at 340/380 nm with emission at 510 nm. Fura-2 fluorescence was recorded with a CCD camera, Cool Snap ES (Roper Scientific/Photometrics). Data were acquired using imaging processing software (IPlab Scanalytic) and analyzed with ImageJ (National Institutes of Health) and Excel (Microsoft). The viability of HEK293 cells was confirmed by responses to 5 μM ionomycin (Sigma-Aldrich).

2.5 Electrophysiology

To measure membrane potentials and currents in HEK293 cells transfected with a desired plasmid DNA, whole-cell patch-clamp recording was used. This technique was utilized to determine the response of TRPA1 to a particular compound, the temperature threshold for heat- or cold-evoked activation and the gating mechanism of mosquito TRPA1 channels. Whole-cell patch-clamp recordings were performed 18 to 30 h after transfection. The extracellular standard bath solution contained 140 mM NaCl, 5 mM KCl, 2 mM $MgCl_2$, 2 mM $CaCl_2$, 10 mM HEPES and 10 mM glucose at pH 7.4 adjusted with NaOH. The intracellular pipette solution contained 140 mM KCl, 5 mM EGTA, and 10 mM HEPES at pH 7.4 adjusted with KOH. HEK293 cells on cover slips were mounted in an open chamber. Chemical stimulation was applied by superfusing a bath solution containing a reagent of interest. Thermal stimulation was applied by increasing the ambient temperature with preheated bath solution. For some experiments that required a varying speed of temperature rise, the length and curvature of perfusion tubes were modified and the height difference between the liquid level and the open chamber was also adjusted to permit more rapid temperature increases. For the experiment of peptide overexpression, 1.63 mg of the 14-amino-acid-long peptide (sequence: MLSVAMYTRKSLRH; molecular weight = 1694.802) was purchased from SCRUM company. The peptide powder was dissolved in dimethyl sulfoxide (DMSO) to make 10 mM

stock solution. The stock solution was further added into the pipette solution for preparing different concentrations. Recording started 2 to 3 min after making a whole-cell configuration for diffusing pipette solution into HEK293 cells to achieve steady state (Oliva et al., 1988). Data were sampled at 10 kHz and filtered at 5 kHz for analysis (Axopatch 200B amplifier with pCLAMP software, Molecular Devices). Membrane potential was clamped at -60 mV and voltage ramp-pulses from -100 to +100 mV (0.5 s) were applied every 5 s.

2.6 Western blotting

2.6.1 Construction of a Myc-tagged plasmid with a double gly-gly-gly-ser linker

In preliminary experiments, we constructed 2 Myc-C-*AgTrpA1*-pcDNA3.1(+) plasmids by ligating *AgTrpA1* inserts with empty 2 Myc-C-pcDNA3.1(+) vectors. *AgTrpA1* inserts were amplified from *AgTrpA1*-pcDNA3.1(+) plasmids. The sequences of the forward and reverse primers were as follows: 5'-CATGCCTACTCCGCTGTACTTAATTCATAG-3' and 5'-TAAGCGGCCGCTCATTTGCCAATAGATTTG-3' for 2 Myc-C-*AgTrpA1Aα* (3759 bp), 5'-CATGTTATCTGTTGCTATGTATACACGC-3' and 5'-TAAGCGGCCGCTCATTTGCCAATAGATTTG-3' for 2 Myc-C-*AgTrpA1Bα(L)* (3639 bp), 5'-CATGTGGCGCAACTGTGCACAAC-3' and 5'-TAAGCGGCCGCTCATTTGCCAATAGATTTG-3' for 2 Myc-C-*AgTrpA1Bα(S)* (3597 bp). The 2 Myc-C-pcDNA3.1(+) vector was digested with EcoRI (NEB), and then the sticky ends were blunted using T4 DNA polymerase (NEB). Later, both insert and vector were digested with NotI (NEB). Finally, linear *AgTrpA1* inserts and linear 2 Myc-C-pcDNA3.1(+) vectors were ligated using Ligation high Ver.2 (TOYOBO).

Linear Myc-tagged *AgTrpA1* plasmids with double gly-gly-gly-ser linkers were directly amplified from 2 Myc-C-*AgTrpA1*-pcDNA3.1(+) plasmids. An extra sequence for coding the

double gly-gly-gly-ser linker was included in the common reverse primer. The sequences of the forward and reverse primers were as follows:

5’- CATGCCTACTCCGCTGTACTTAATTCATAG-3’ and 5’-GAGCCGCCTCCGCTTCCGCCTCCCAAGTCCTCTTCAGAAATGAGCTTTTGCTCCATATCAAGCTTCAAGTCC-3’ for 2 Myc-C-linker-*AgTrpA1Aa* (9222 bp), 5’-CATGTTATCTGTTGCTATGTATACACGC-3’ and 5’-GAGCCGCCTCCGCTTCCGCCTCCCAAGTCCTCTTCAGAAATGAGCTTTTGCTCCATATCAAGCTTCAAGTCC-3’ for 2 Myc-C-linker-*AgTrpA1Ba(L)* (9102 bp), 5’-CATGTGGCGCAACTGTGCACAAC-3’ and 5’-GAGCCGCCTCCGCTTCCGCCTCCCAAGTCCTCTTCAGAAATGAGCTTTTGCTCCATATCAAGCTTCAAGTCC-3’ for 2 Myc-C-linker-*AgTrpA1Ba(S)* (9060 bp). These linear plasmid PCR products were treated with T4 Polynucleotide Kinase (NEB) and self-ligated using Ligation high Ver.2 (TOYOBO).

2.6.2 Protein isolation

HEK293 cells in a 10-cm dish were transfected with 4 μg of plasmid DNA and incubated overnight. Whole cell extracts of HEK293T cells were collected by scraping in RIPA lysis buffer (Cell Signaling Technology). Cytosolic and membrane fractions were isolated using a subcellular protein fractionation kit according to the manufacturer’s protocol (Thermo Fisher Scientific). Protein concentration was quantified with the Lowry assay (Bio-Rad), and a standard curve was prepared with 5 μL of different dilutions of BSA (0, 1.25, 2.5, 5 and 10 μg/μL diluted in RIPA buffer). The absorbance of protein samples was used to fit the calibration curve to quantify protein concentration with a Nanodrop (Thermo Fisher Scientific). Proteins (30 μg) from whole cell, cytosolic and membrane fractions were used.

These proteins were denatured with 4x Laemmli Sample Buffer (Bio-Rad) and 100 mM DTT at 95°C for 5 min before resolution using an 8% SDS-PAGE gel.

2.6.3 Plasma membrane protein biotinylation

HEK293 cells in a 3.5-cm dish were transfected with 1 μg plasmid DNA and incubated overnight. The HEK293 cells were washed with PBS and incubated twice with 0.5 mg/mL EZ-link-NHS-LC-Biotin (Abcam) for 10 min each. Cells were washed with quenching buffer (100 mM glycine in PBS, pH 7.3) and washed with PBS. Cells were collected and lysed in 1x TNE buffer with 1% NP-40 and complete protease inhibitor cocktail (lysis buffer). Biotinylated proteins were precipitated overnight using 10 μL Dynabeads MyOne Streptavidin T1 (Thermo Fisher Scientific) with agitation at 4°C. Beads were washed 3 times with 100 μL lysis buffer at room temperature. Beads (10 μL) and eluates were denatured with 2x Laemmli Sample Buffer (Bio-Rad) and 100 mM DTT at 95°C for 5 min before resolution on a 6% SDS-PAGE gel.

2.6.4 Western blot and normalization of relative protein amount

For Western blot experiments, electrophoresis was run at 120 mV for 1.5 hours. The SDS-PAGE gel was then transferred to a mini format, 0.2 μm PVDF membrane with Trans-Blot Turbo (Bio-Rad) for 10 min (25 V, 1.3 A). Non-specific sites were blocked by incubating the membrane in PBS-T containing 3% BSA. Primary antibodies were used to incubate the membrane overnight. They included: anti-Myc (MBL Life science): 1/5000; anti-β-actin (Sigma-Aldrich): 1/2000 diluted in PBS-T containing 1.5% BSA for isolated protein samples; anti-Myc: 1/1000 diluted in PBS-T containing 1.5% BSA for biotinylated protein samples). Secondary antibody was incubated with the membrane for 1 h (anti-mouse HRP (Cell Signaling Technology): 1/1000 diluted in PBS-T containing 1.5% BSA). Protein bands were detected with

the use of Amersham ECL Prime Western Blotting Detection Reagent (GE Healthcare) and a LAS-3000 mini image analyzer (Fujifilm). Quantification of Western blot bands was performed using Image J software (National Institutes of Health).

2.7 Chemicals

To test the chemosensitivity of mosquito TRPA1, the most common TRPA1 ligand allyl isothiocyanate (AITC) and the well-known natural mosquito repellent citronellal were utilized in most experiments. Both compounds were dissolved in DMSO to make 1 M stock solutions.

To screen potential mosquito TRPA1 agonists, the following 23 compounds were tested: **1**. α-Terpineol, **2**. Nerol, **3**. Carvacrol, **4**. 2-(2-Butoxyethoxy) ethyl acetate (2-BEA), **5**. Linalool, **6**. Limonene, **7**. Citral, **8**. β-Caryophyllene, **9**. 3,7-Dimethyl-6-Octenal, **10**. Diallyl Disulfide, **11**. decanal. **12**. octanal, **13**. nonanal, **14**. lauric acid, **15** undecanoic acid, **16**. decanoic acid, **17**. nonanoic acid, **18**. octanoic acid, **19**. hexanoic acid, **20**. heptanoic acid, **21**. butyric acid, **22**. valeric acid and **23**. propionic acid. These compounds were dissolved with organic solvents to make 1 M stock solutions (except for β-Caryophyllene stock solution that was made 0.91 M). β-Caryophyllene was dissolved with 91% DMSO + 9% Ethanol. Compound numbers **11**-**23** were dissolved with 100% ethanol. The rest of the compounds were dissolved with 100% DMSO.

2.8 Statistical analysis

Data are presented as means $\pm$ standard error of mean (S.E.M). Statistical analysis was performed by unpaired Student's *t*-test. Statistical significance is defined as: *, $p < 0.05$; **, $p < 0.01$ and ***, $p < 0.001$.

CHAPTER 3

Results

3.1 Cloning and identification of TrpA1 variants from Anopheles gambiae, Anopheles stephensi, Aedes aegypti and Culex pipiens pallens

To identify the splicing variants of *TrpA1* genes, we performed 5'- and 3'-RACE to identify the most upstream and downstream exons that coded protein. First, the genomic sequences of target mosquito species were examined to design PCR primers for the 5'- and 3'-RACE. The amplified PCR products obtained by 5'-RACE were sequenced to identify the splicing variants of TRPA1 and potential initiation codons for each splicing variant were identified afterwards. The PCR products of 3'-RACE were also sequenced to identify the termination codons. Finally, PCR primers for amplifying entire coding regions of each splicing variant were designed.

As a result, several different splicing variants were identified (Fig. 1.1). Similar to *Drosophila TrpA1*, alternatively spliced exons at the N-terminus and in the middle of the *TrpA1* gene were found. In the present study, upstream or downstream exons are designated as "A" and "B", respectively. In addition, the N-terminal and middle portions of alternative splicing exons are designated with uppercase and lowercase letters, respectively (Fig. 1.1). Two splicing variants of *AgTrpA1* cloned by Kang et al (2012) were named *TrpA1Aa* and *TrpA1Ba* in the present study. Nevertheless, examination of a genomic sequence database of *Anopheles gambiae* revealed the exon corresponding to "b" in the middle of the *TrpA1* gene, suggesting that it was potentially included in the transcripts. In addition, *TrpA1* was newly cloned from *Anopheles stephensi*, *Anopheles aegypti* and *Culex pipiens pallens* in the present study. Two kinds of splicing variants were identified from *Anopheles stephensi* and *Culex pipiens pallens* (*TrpA1Ab* and *TrpA1Ba*). Moreover, 3 kinds of splicing variants were identified from *Aedes aegypti* (*TrpA1Ab*, *TrpA1Ba*, and *TrpA1Bb*) (Fig. 1.1).

In the course of cloning procedures, I found that the N-terminal regions of previously reported AgTRPA1B and AaTRPA1B were truncated. As shown in Figure 1.2 and 1.3,

methionines were found 14 amino acids upstream of previously reported methionine by Kang et al (2012) in *Anopheles gambiae* and *Aedes aegypti*. A methionine was also found 9 amino acids upstream of a previously reported methionine in *Culex pipiens pallens.* Notably, these newly found methionine codons are located upstream of a previously reported one in the same reading frame; and these methionine codons are also in the vicinity of the upstream termination codons (Fig. 1.3). In addition, newly identified portions were well conserved among the 4 species. Thus, it is highly possible that these additional amino acids exist in the mosquito TRPA1 (Fig. 1.2 and 1.3). Therefore, truncated TRPA1(B) reported by Kang et al (2012) is designated as TRPA1B(S), and TRPA1B with newly identified amino acids in the N-terminus is designated as TRPA1B(L) when comparing these 2 different clones in later sections. Otherwise, I designated TRPA1B as TRPA1B(L) when it was used in electrophysiological experiments.

Figure 1: Identification of *TrpA1* variants from *Anopheles gambiae, Anopheles stephensi, Aedes aegypti* and *Culex pipiens pallens*

1.1 a

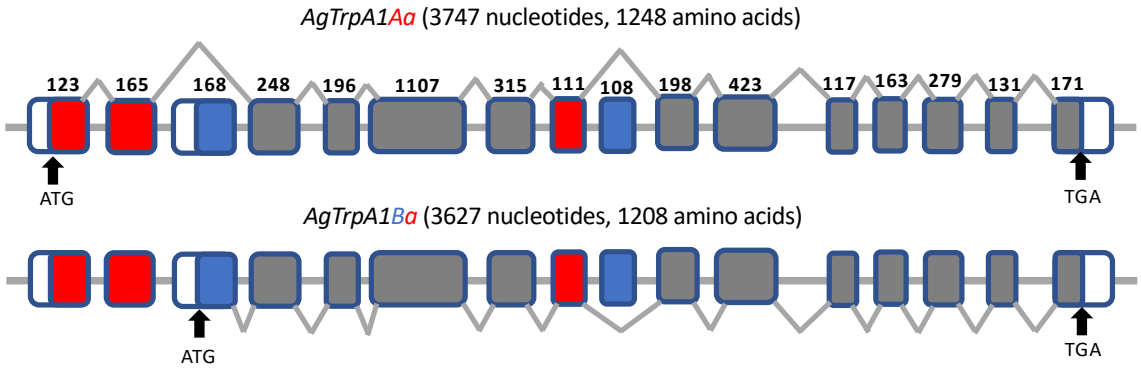

1.1 b

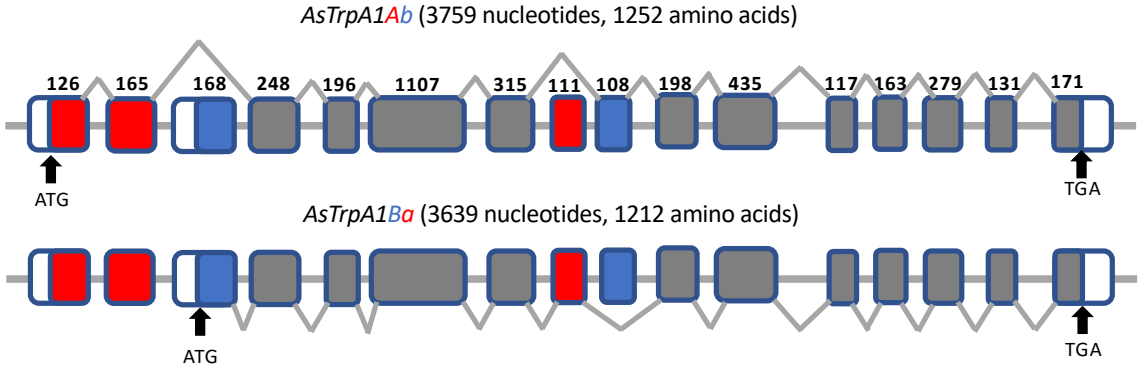

1.1 c

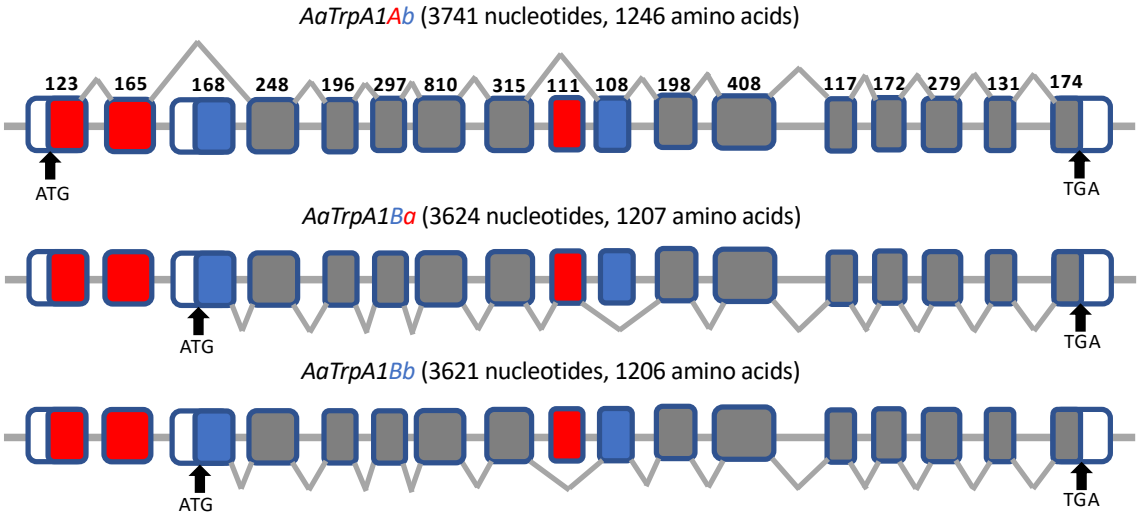

1.1 d

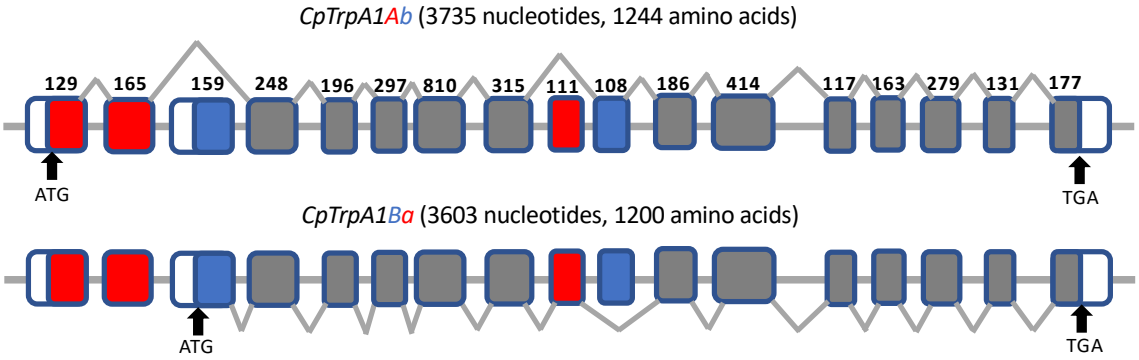

Figure 1.1 Schematic exon-intron structures of *TrpA1* variants of disease vector mosquitoes.

The naming of different splicing variants is based on the new nomenclature. (a) *AgTrpA1Aa* and *AgTrpA1Ba*. (b) *AsTrpA1Ab* and *AsTrpA1Ba*. (c) *AaTrpA1Ab*, *AaTrpA1Ba* and *AaTrpA1Bb*. (d) *CpTrpA1Ab* and *CpTrpA1Ba*.

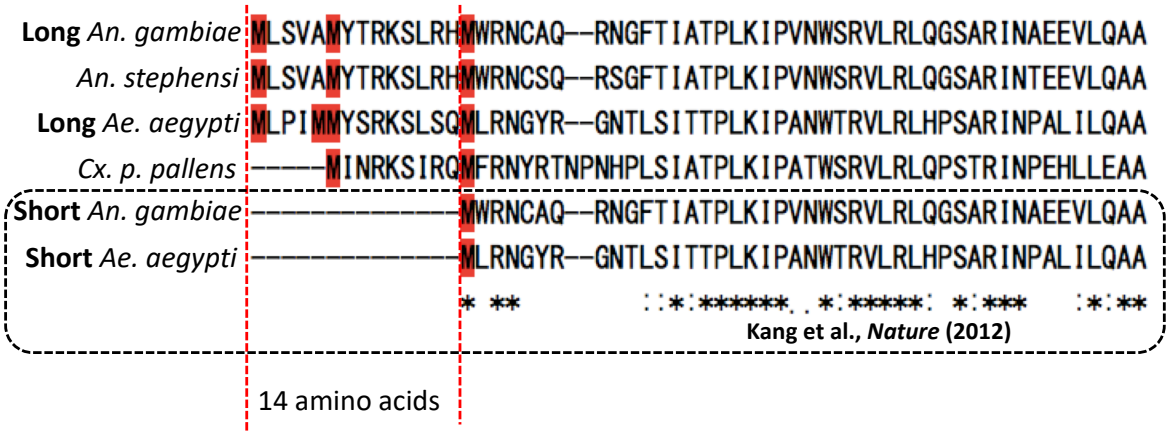

Figure 1.2 Amino acid sequence alignment of the N-terminus of mosquito TRPA1(B). Black dash line cycled amino acid sequences were reported by Kang et al in 2012.

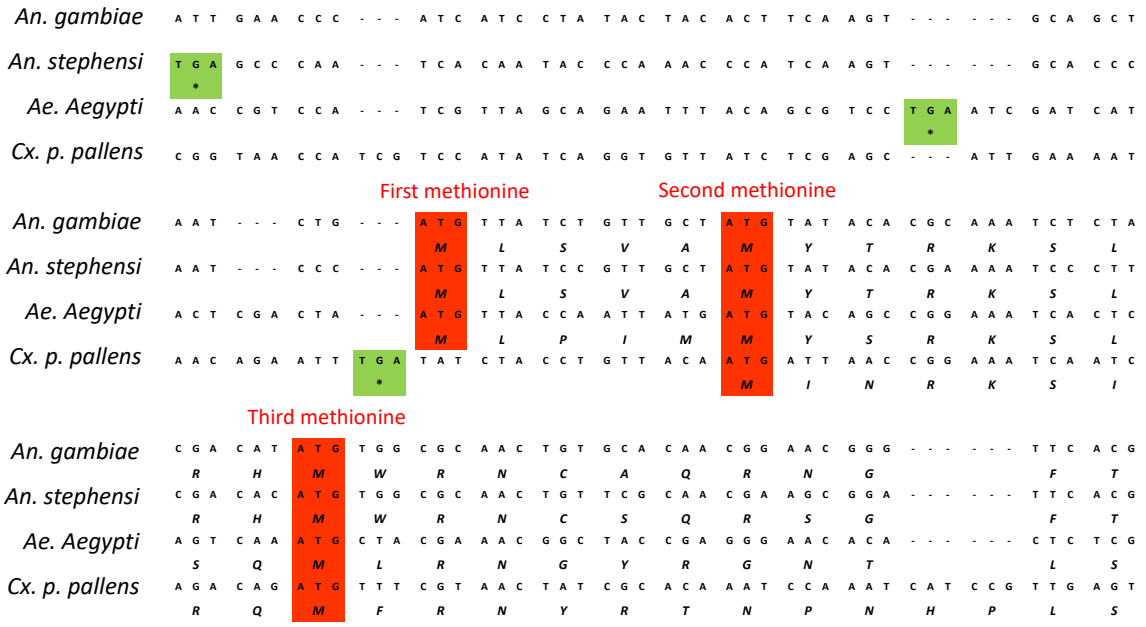

Figure 1.3 DNA sequence alignment of the beginning of *TrpA1(B)* from 4 mosquito species (genomic sequence of *Anopheles gambiae*, 5' RACE result of the other 3 species). Methionine codons are red highlighted, and the upstream stop codons are green highlighted.

3.2 The temperature threshold for heat activation was not affected by the rate of temperature increase

The purpose of the present study was to compare the thermal responses of splicing variants of TRPA1 from 4 different species. However, before starting such a comparative analysis, I examined whether the speed of the heat ramp affected the thermal responses of mosquito TRPA1, including activity (the current density) and sensitivity (temperature threshold for activation). AgTRPA1Ba(S) was used for this purpose since it was reported to be activated by heat stimulation in a previous study (Kang et al, 2012). AgTRPA1Ba(S) was transiently expressed in HEK293 cells and whole-cell ionic currents against heat stimulation were measured. Since the temperature threshold for activation of AgTRPA1Ba(S) was reported to be 24.8 °C (Kang et al. 2012), the temperature of the bath solution was cooled down to about 15°C prior to heat stimulation (Fig. 2.1). The rates of heat ramps were changed, and the current density and temperature threshold for activation were calculated from heat-evoked ionic currents obtained from AgTRPA1Ba(S) expressed in HEK293 cells. The speed was calculated by measuring the time for a linear 10^{o}C temperature rise (Fig. 2.1). Figure 2.2 shows that the current density of AgTRPA1Ba(S) to heat stimulation was increased with the speed of heat increase, while its temperature threshold for activation was not affected. These observations clearly indicated that the heat ramp speed should be constant throughout my investigation. Therefore, all the heat-stimulation experiments in this project followed the protocol with a temperature increase speed of approximately 1.5^{o}C/sec.

Figure 2 Effect of the rate of temperature change in the heat-activation of mosquito TRPA1

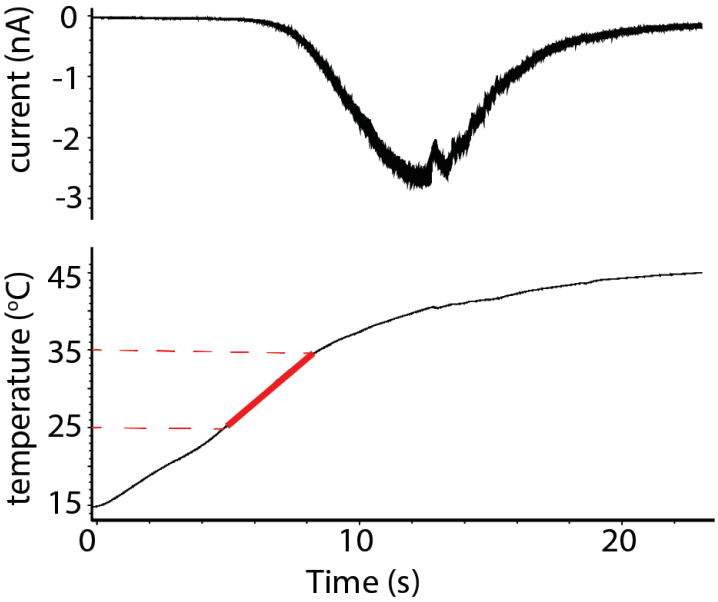

Figure 2.1 Heat-evoked currents recorded from HEK293 cells expressing AgTRPA1Ba(S). An example of a linear 10°C temperature rise during TRPA1 activation (highlighted with red color in the temperature trace).

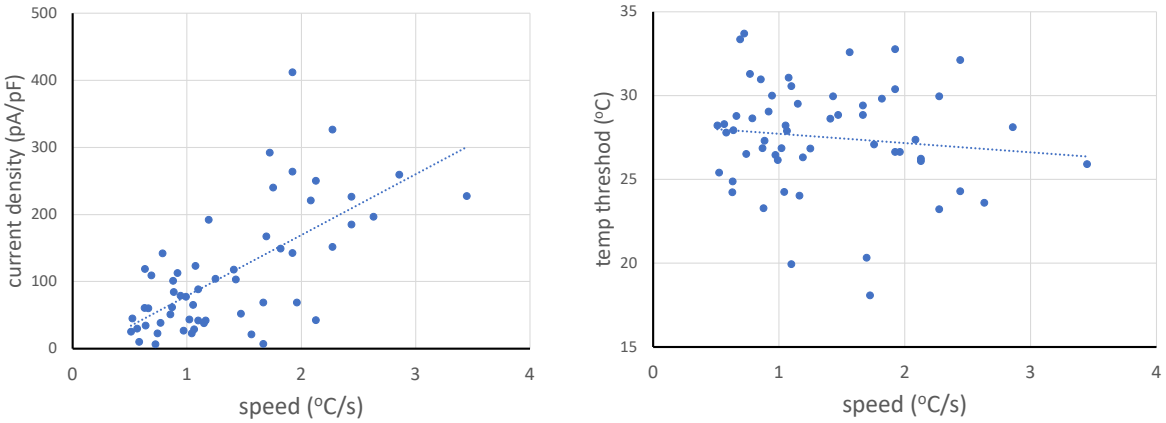

Figure 2.2 The relevance between current density or temperature threshold for heat activation and temperature increase rate at 2 different basal temperature. At a basal temperature of 15°C, there was a positive correlation between the rate of temperature increase and the heat-evoked current density. In addition, there was a slightly negative correlation between the rate of temperature increase and the temperature threshold for heat activation. All the data were recorded and measured from HEK293 cells expressing AgTRPA1Ba(S).

3.3 Addition of 14 amino acids to the TRPA1B N-terminus attenuated the channel activity

It appeared that AgTRPA1Aa and AgTRPA1Ba showed distinct channel sensitivities to heat stimuli. I hypothesized that the differences in sensitivities might be due to differences in the N-termini (Kang et al., 2012) and that such differences might determine specific channel properties observed in TRPA1B channels with or without a short peptide at the N-terminus. Therefore, I investigated whether the additional 14 amino acids in the N-termini of AgTRPA1Ba and AaTRPA1Ba played an important role in modulating channel properties. The activities of TRPA1Ba(S) and TRPA1Ba(L) were compared in *Anopheles gambiae* (Fig. 3 a & b) and *Aedes aegypti* (Fig. 3 c & d). With application of heat stimuli or high concentrations of citronellal, the maximal currents were recorded and the current densities were compared. Surprisingly, the addition of 14 amino acids to the N-terminus of TRPA1Ba significantly attenuated the density of heat- and citronellal-evoked currents in both mosquito species. From comparative sequence analysis shown in Figure 1, TRPA1Ba(L) is likely to exist in mosquito species. Therefore, I used TRPA1Ba(L) in all 4 mosquito species in further electrophysiological experiments.

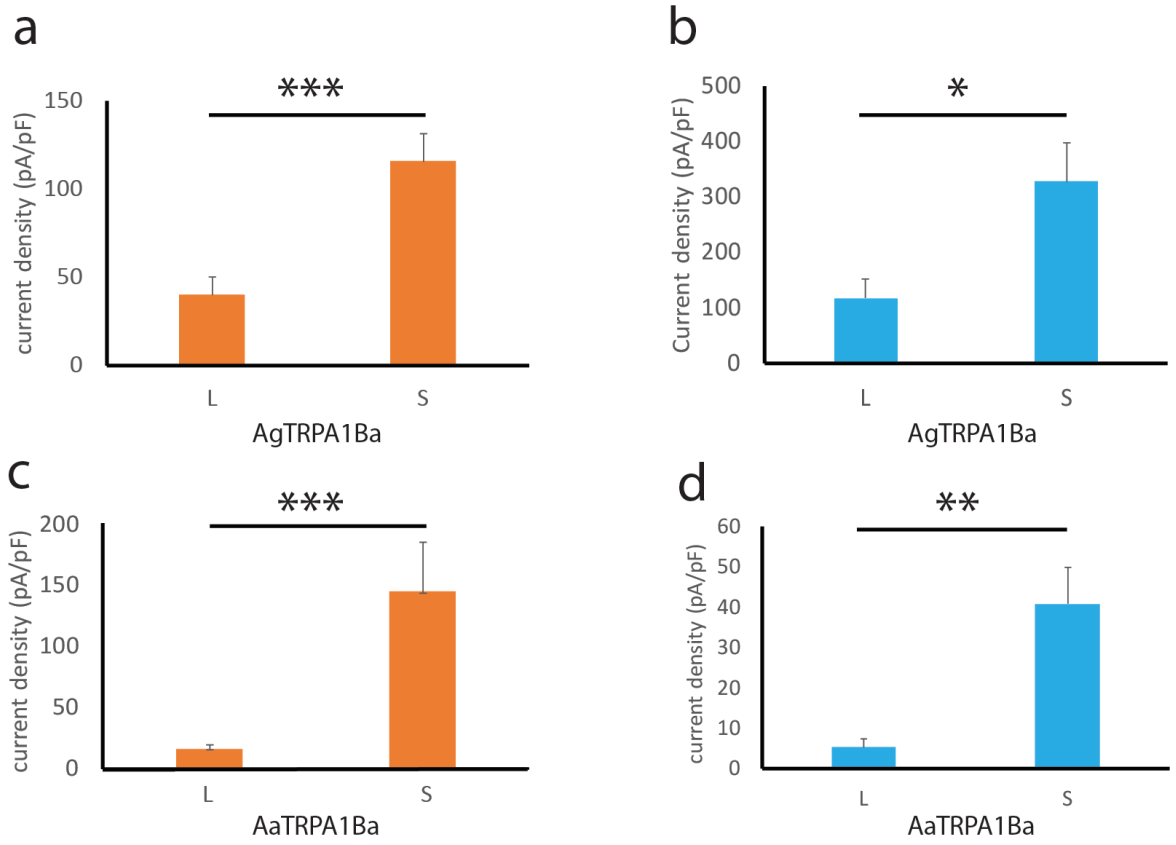

Figure 3 Effects of an additional 14 amino acids at the N-terminus of TRPA1Ba on channel properties. Heat-induced current (a) and 5 mM citronellal-evoked current (b) were recorded from naïve HEK293 cells expressing AgTRPA1Ba(S) or AgTRPA1B(L); heat-induced current (c) or 3 mM citronellal-evoked current (d) were recorded from naïve HEK293 cells expressing AaTRPA1Ba(S) or AaTRPA1B(L). In both *Anopheles gambiae* and *Aedes aegypti*, TRPA1Ba(L) generated significantly reduced heat or chemically evoked currents compared with TRPA1Ba(S). All values are means ± S.E.M; n ⩾ 5; *, $P < 0.05$; **, $P < 0.01$; ***, $P < 0.001$.

3.4 Including 14-amino-acid-long peptide into pipette solution did not change the channel activity.

Given that channel activity was low when the 14 amino acids were added to the N-terminus of TRPA1Ba (section **3.3**). I wondered by which mechanism such a short peptide could affect the channel activity of TRPA1. I therefore dissolved this peptide into pipette solution to achieve different intracellular concentrations to mimic the circumstance that the peptide is overexpressed in HEK293 cells expressing AgTRPA1Ba(S). I maintained the intracellular concentrations of this peptide at different levels, 1 μM, 10 μM or 100 μM in a whole-cell mode, and then measured the size of heat-evoked current. Intriguingly, addition of this 14-amino-acid-long peptide in HEK293 cells did not cause any significant change in the density of heat-evoked currents. Moreover, the densities of heat-evoked currents were still significantly larger than the ones recorded from HEK293 cells expressing AgTRPA1Ba(L) (Fig. 4). As a result, I thought that smaller currents evoked by heat in the cells expressing AgTRPA1Ba(L) were not caused by the binding of the 14 amino acids to the channel.

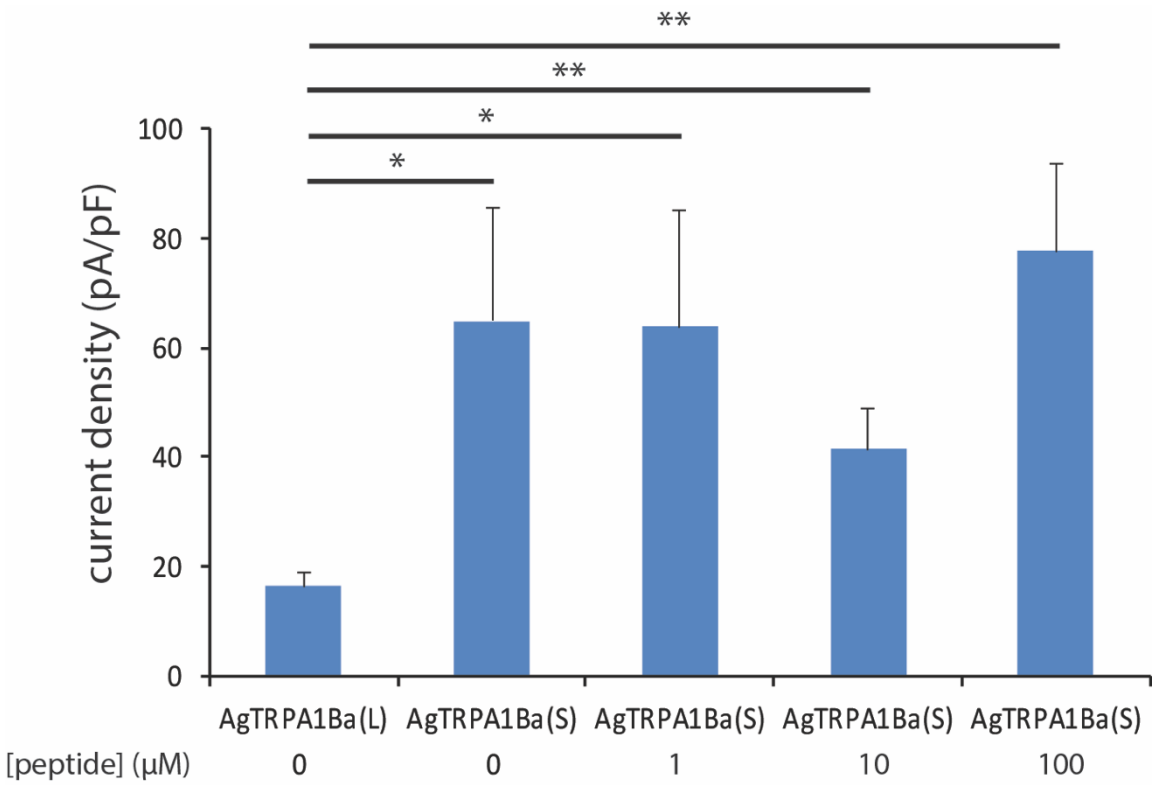

Figure 4 Effects of intracellularly diffusing dissociative 14-amino-acid-long peptide on thermosensitivity of AgTRPA1Ba(S). Heat-evoked currents were recorded from naïve HEK293 cells expressing AgTRPA1Ba(L) or AgTRPA1Ba(S) with a certain concentration of dissociative 14-amino-acid-long peptide intracellularly. Adding 1 μM, 10 μM or 100 μM peptide into HEK293 cells expressing AgTRPA1Ba(S) did not significantly affect heat evoked currents, while the densities of the currents evoked by heat remained significantly larger than that of AgTRPA1Ba(L). All values are means ± S.E.M; n ⩾ 8; *, $P < 0.05$; **, $P < 0.01$.

3.5 A short alternative splicing exon between ankyrin repeats and the transmembrane domain is not important for AaTRPA1 temperature sensing

Among 4 mosquito species, 2 different TRPA1B isoforms were solely identified in *Aedes aegypti*. The difference between AaTRPA1Ba and AaTRPA1Bb is an amino acid stretch that is 37 or 36 amino acids long in the intracellular region that is located between the last ankyrin repeat and the first transmembrane segment (Fig. 1.1 c). This structure resembles the alternative splicing variants of TRPA1 found in *Drosophila melanogaster*. In *Drosophila*, this intracellular region has been reported to be critical for TRPA1 responses to heat stimuli (Zhong et al., 2012). Therefore, the effects of a single alternative splicing exon of TRPA1B (TRPA1Ba and TRPA1Bb) to heat stimulation were examined in *Aedes aegypti*. Calcium-imaging experiments with Fura-2 were employed to check the responses of AaTRPA1Ba and AaTRPA1Bb to heat stimuli. The 2 channels responded similarly to heat stimulation (Fig. 5.1). To compare their activities in detail, the current densities against heat stimulation were compared using a whole-cell patch-clamp method. There was no significant difference between these 2 splice variants (Fig. 5.2). Hence, the amino acids located near the first transmembrane domain do not appear to have significant roles regarding the activity of TRPA1 in *Aedes aegypti.* In later experiments, AaTRPA1Bb was mainly used for comparison with other TRPA1 variants.

Figure 5 AaTRPA1Ba and AaTRPA1Bb possess similar thermosensitivity.

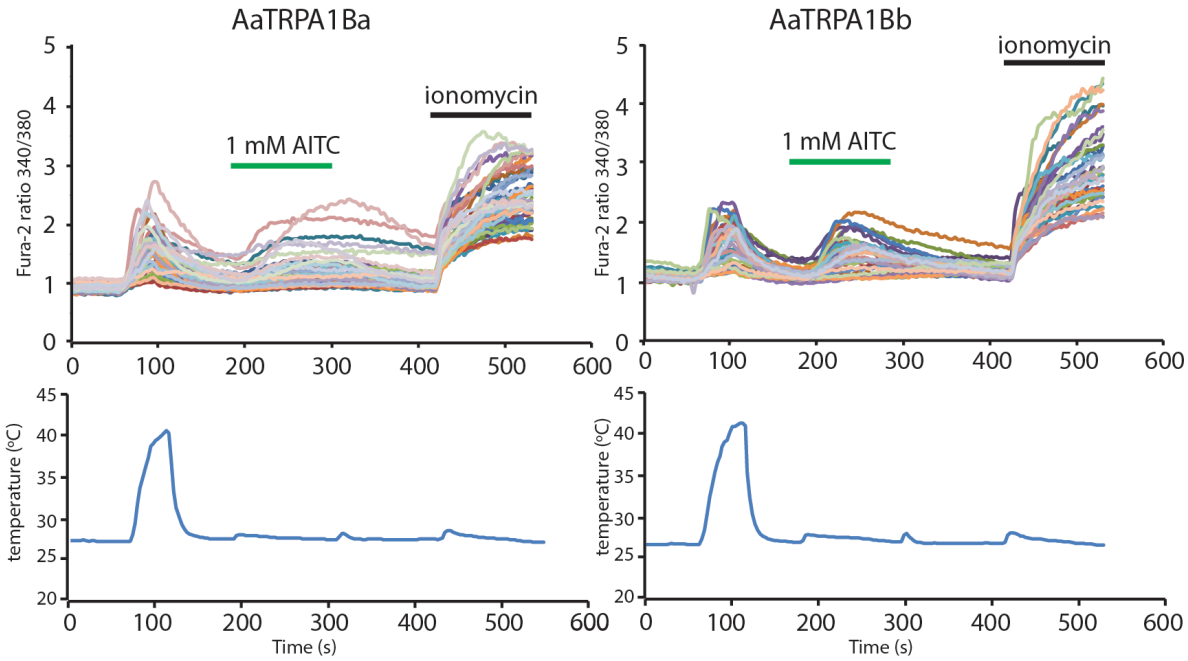

Figure 5.1 Fura-2 calcium-imaging testing the heat responses of AaTRPA1Ba and AaTRPA1Bb. HEK293 cells expressing AaTRPA1Ba and AaTRPA1Bb were subjected to a hot bath solution to elevate the temperature from room temperature to near 42°C. Blue traces represent the real-time temperature change during calcium-imaging. One min after heat stimulation, 1 mM AITC (green bar) was applied for 2 min as a positive control. Ionomycin (5 μM) (black bar) was applied in the last 2 min to confirm the viability of HEK293 cells.

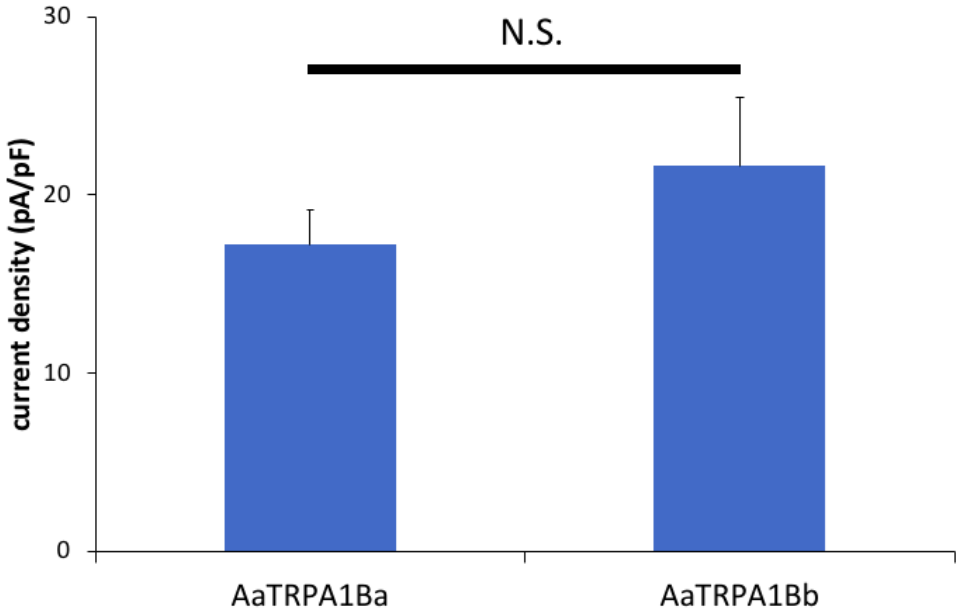

Figure 5.2 Whole-cell patch-clamp recording testing heat responses of AaTRPA1Ba and AaTRPA1Bb. Quantification of current densities activated by increasing bath solution temperature from 15°C to near 42°C using HEK293 cells expressing AaTRPA1Ba or AaTRPA1Bb in whole-cell patch-clamp recording. No significant difference was found. All values are means ± S.E.M, n = 9 for AaTRPA1Ba, n = 21 for AaTRPA1Bb.

3.6 Splicing variants of mosquito TRPA1 showed distinct thermal responses.

The alternative splicing in the middle linker region of TRPA1 did not alter the activity of AaTRPA1 (section **3.5**). Thus, the significance of the N-terminal difference was investigated in this section. I first compared the density of the currents evoked by heat. TRPA1B showed much larger current densities than those of TRPA1A from *Anopheles gambiae*, *Anopheles stephensi* and *Culex pipiens pallens*, but not from *Aedes aegypti*. Among them, the current density of CpTRPA1Ba was the largest (Fig. 6 a). Moreover, temperature thresholds for heat-evoked activation of each mosquito TRPA1B were compared because temperature thresholds for heat evoked TRPA1A currents were too small to be analyzed. Three tropical mosquito species, *Anopheles gambiae*, *Anopheles stephensi* and *Aedes aegypti* had similar temperature thresholds of 28.5 $\pm$ 0.7, 30.3 $\pm$ 0.9 and 32 $\pm$ 0.8^{o}C, respectively. The sole mosquito species living in the temperate zone, *Culex pipiens pallens*, collected in Nara Prefecture, had a remarkably low temperature threshold of 21.8 $\pm$ 0.7^{o}C (Fig. 6 b).

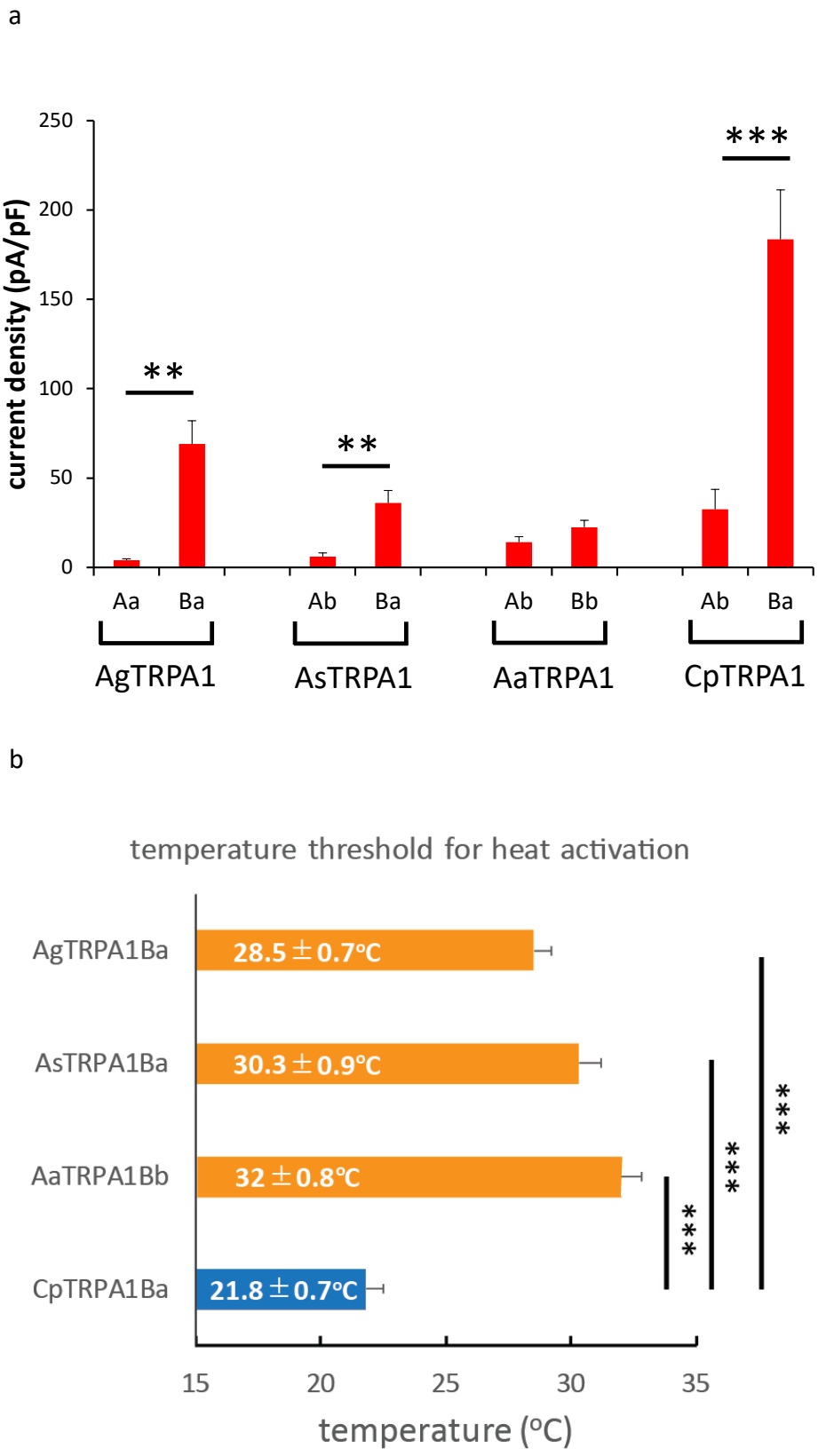

Figure 6 Divergent thermosensitivities of TRPA1 variants among different mosquito species.

(a) Quantification of current densities activated by increasing bath solution temperature from

15°C to near 42°C using HEK293 cells expressing AgTRPA1Aa, AgTRPA1Ba, AsTRPA1Ab, AsTRPA1Ba, AaTRPA1Ab, AaTRPA1Bb, CpTRPA1Ab or CpTRPA1Ba. TRPA1 variants from the same species were closely ranged. (b) Average temperature thresholds for heat activation were measured and calculated from the current traces of AgTRPA1Ba, AsTRPA1Ba, AaTRPA1Bb and CpTRPA1Ba. Means ± S.E.M of temperature threshold for heat activation are labeled on the corresponding bars of the chart. $10 \leqslant n \leqslant 60$ each; **, $P < 0.01$; ***, $P < 0.001$.

3.7 Splicing variants of mosquito TRPA1 also showed different chemical responses.

AITC and citronellal are TRPA1 agonists that reportedly induce feeding deterrence in *Drosophila melanogaster* through activation of TRPA1 (Kang et al., 2010; Du et al., 2015). Here, I investigated the effects of these 2 compounds on splicing variants of multiple mosquito TRPA1s by expressing them in HEK293 cells. Increasing concentrations of AITC (0.008 to 1 mM) or citronellal (0.1 to 3 mM) were applied to HEK293 cells expressing each splicing variant from 4 mosquito species. There was no apparent difference in the sensitivity to the 2 chemicals in the examined mosquito TRPA1s. Those data are consistent with the fact that both chemicals are electrophiles except for AaTRPA1Ab in which 1 mM AITC-induced currents were smaller than those induced by 0.2 mM AITC. It could be partly explained by desensitization because AITC induced large current responses. The more detailed comparative analyses demonstrated that AgTRPA1Aa and AgTRPA1Ba showed similar sensitivities to both chemicals, whereas the chemical sensitivity of AsTRPA1Ab was lower than that of AsTRPA1Ba (Fig. 7). On the other hand, TRPA1Ab of *Aedes aegypti* and *Culex pipiens pallens* exhibited higher sensitivities to both chemicals than AaTRPA1Bb and CpTRPA1Ba. When the sensitivities of both splicing variants of TRPA1 were combinatorically compared among species, TRPA1 of *Aedes aegypti* and *Culex pipiens pallens* had much higher sensitivities compared to those of *Anopheles gambiae* and *Anopheles stephensi*. These data suggested that *Aedes aegypti* and *Culex pipiens pallens* experienced similar evolutionary paths that were different from those of *Anopheles gambiae* and *Anopheles stephensi*. Indeed, a phylogenic tree of mosquitoes (Kamali et al., 2014) supports this idea.

a

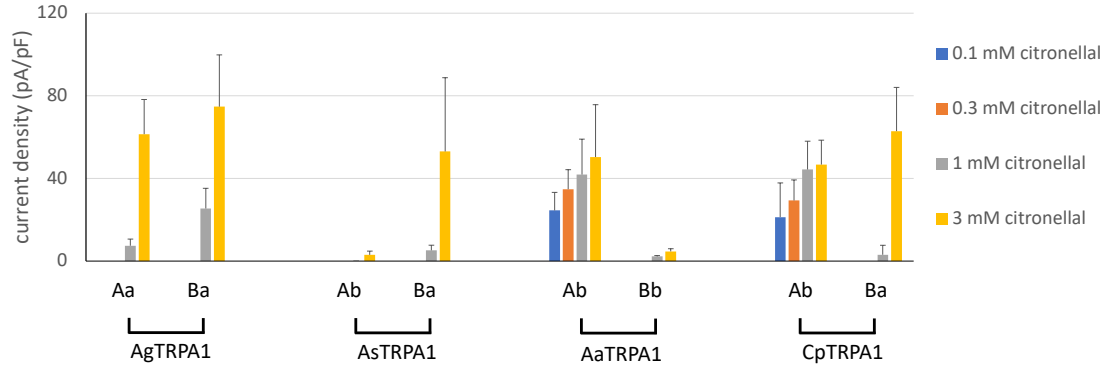

b

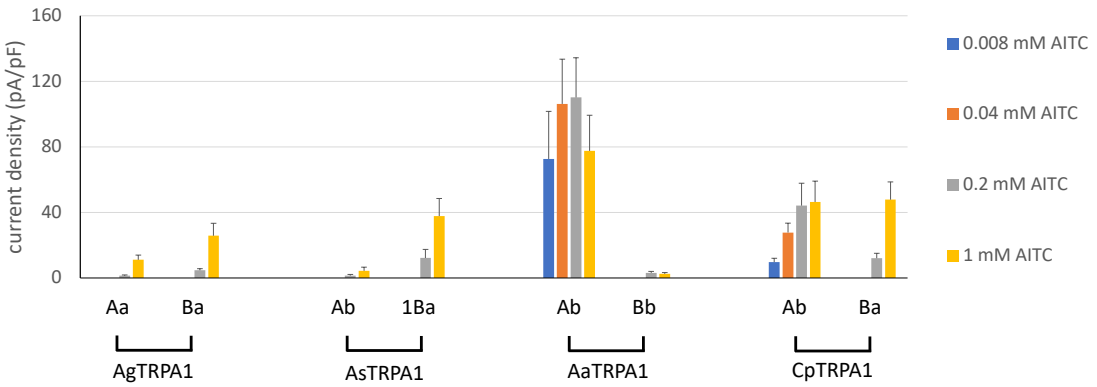

Figure 7 Comparison of chemosensitivities among TRPA1 variants and orthologues of mosquitoes (a) Quantification of TRPA1-mediated current densities activated by 0.1, 0.3, 1 or 3 mM citronellal. (b) Comparison of TRPA1-mediated current densities activated by 0.008, 0.04, 0.2 or 1 mM AITC. All values are means ± S.E.M, $5 \leqslant n \leqslant 12$ each.

3.8 Western blotting analysis of the expression levels of AgTRPA1 in HEK293 cells

As shown in the above sections, splicing variants of TRPA1 showed variable responses to chemical and heat stimuli. These differences could result from both the variations in the expression levels on the cell membrane and/or channel properties of splicing variants of TRPA1. To quantify the amounts of TRPA1 proteins, Western blotting analyses were performed. It was not feasible to examine the expression levels in HEK293 cells for all the identified splicing variants of mosquito TRPA1. Therefore, I chose 3 representative TRPA1 variants of *Anopheles gambiae* (AgTRPA1Aa, AgTRPA1Ba(L) and AgTRPA1Ba(S)) for the comparison of expression levels. First, Myc-tagged *AgTrpA1* plasmids were constructed. Then, 2 Myc tags were added at the N-terminus of each TRPA1 channel protein. And, a double gly-gly-gly-ser linker was added between the AgTRPA1 N-terminus and 2 Myc tags to avoid effects of folding in the secondary structure (Fig. 8.1).

In the Western blotting experiments, the amounts of protein in the extracts from whole cells, cytoplasm and membranes of AgTRPA1Aa, AgTRPA1Ba(L) and AgTRPA1Ba(S) were examined. AgTRPA1 with a molecular weight of approximately 130 KDa was detected with an antibody against Myc (Fig. 8.2 a). The amount of AgTRPA1 proteins was normalized to those of β-actin (~42 KDa) for comparison. With the integrated data from 3 independent Western blotting experiments, TRPA1/β-actin ratios of different cellular portions were determined. Protein amounts of AgTRPA1Aa and AgTRPA1Ba(S) were similar whereas that of AgTRPA1Ba(L) tended to be lower than those of the former 2 splicing variants in the extracts. To examine the effects of addition of Myc at the N-terminus of TRPA1 on channel properties, currents of Myc-tagged AgTRPA1 channels were compared with those of untagged AgTRPA1. Heat or a high concentration of citronellal was applied to HEK293 cells expressing each AgTRPA1 channel, and maximum peak currents were compared. Quantified peak current densities

were summarized not only for comparing the significance of adding Myc-tags, but also for comparing the correlation between current densities and expression levels revealed in the Western blotting analyses. No significant difference between Myc-tagged AgTRPA1 and untagged AgTRPA1 was observed in the citronellal-evoked currents (Fig. 8.3 a). On the other hand, the densities of heat-evoked currents for Myc-tagged AgTRPA1Ba(L) were significantly larger than those for the untagged one. Such a significant alteration of thermosensitivity was not found in either Myc-tagged AgTRPA1Aa or Myc-tagged AgTRPA1Ba(S) (Fig. 8.3 b).

Figure 8 Expression levels of variants of AgTRPA1 in HEK293 cells analyzed with western blotting.

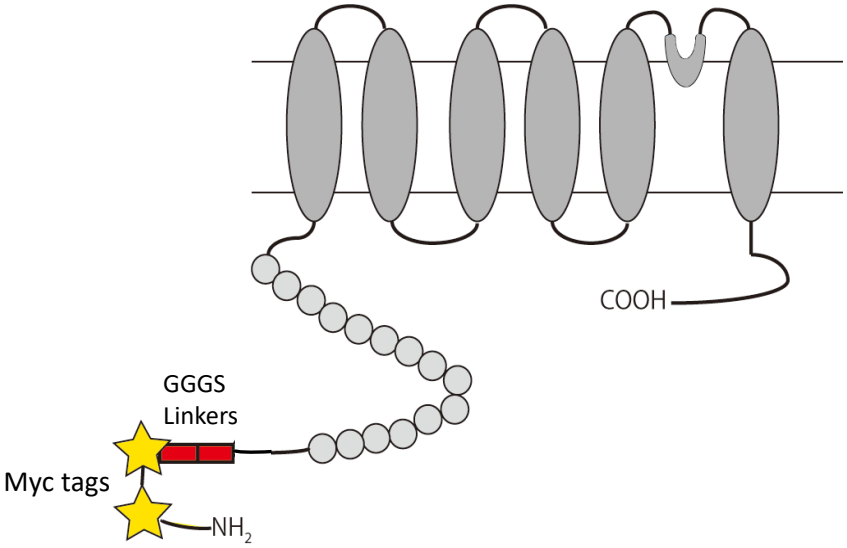

Figure 8.1 A schematic depiction of Myc-tagged TRPA1 channel protein. Grey colored domains belong to the original TRPA1. Each red rectangle represents a gly-gly-gly-ser linker. Each yellow five-pointed star represents a 10 amino-acid-long Myc sequence.

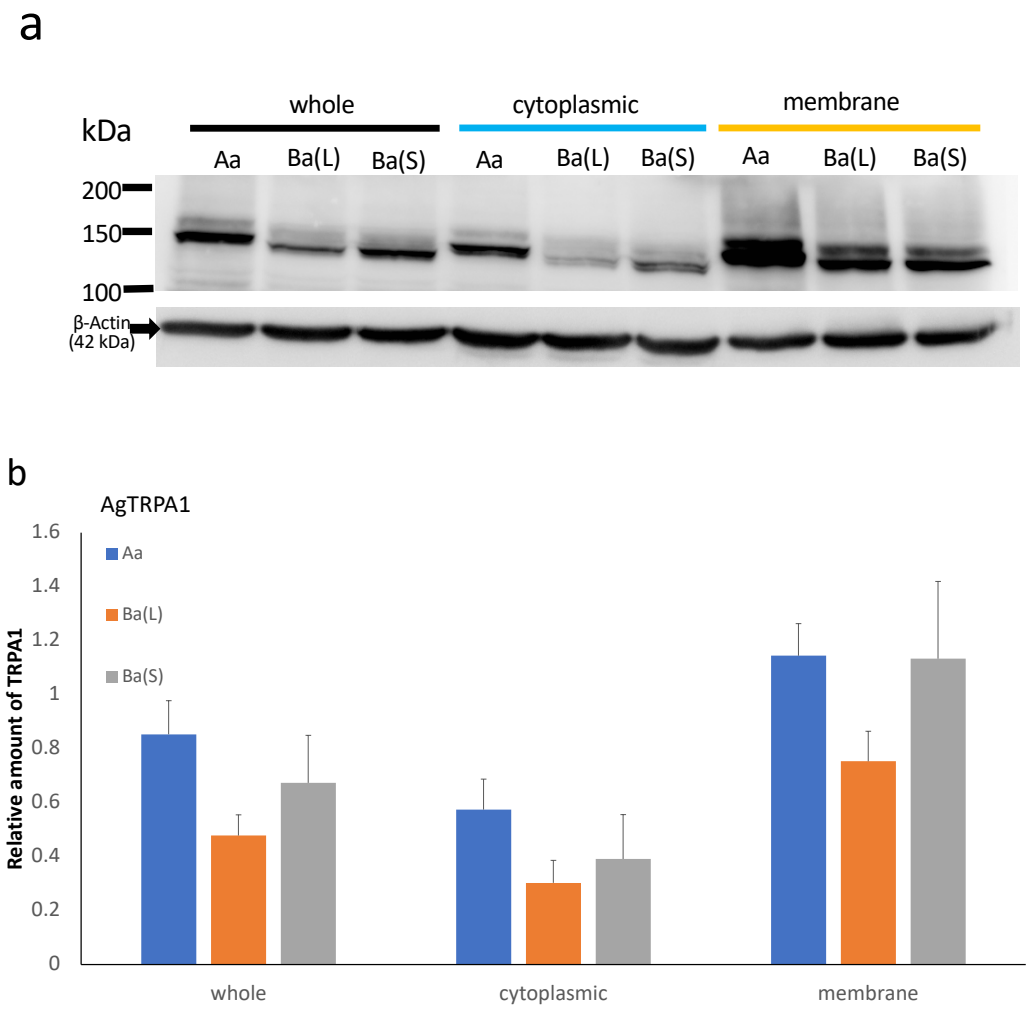

Figure 8.2 Quantification of the amounts of protein for AgTRPA1Aa, AgTRPA1Ba(L) and AgTRPA1Ba(S) in HEK293 cells. (a) Proteins were extracted from HEK293 cells transfected with vectors containing AgTRPA1 tagged with Myc sequences at the N-terminus. Proteins were extracted from whole cells, cytoplasm and membrane. AgTRPA1 was detected with antibody against Myc. (b) The amounts of AgTRPA1 protein were normalized to those of β-actin. All values are means ± S.E.M, n = 3.

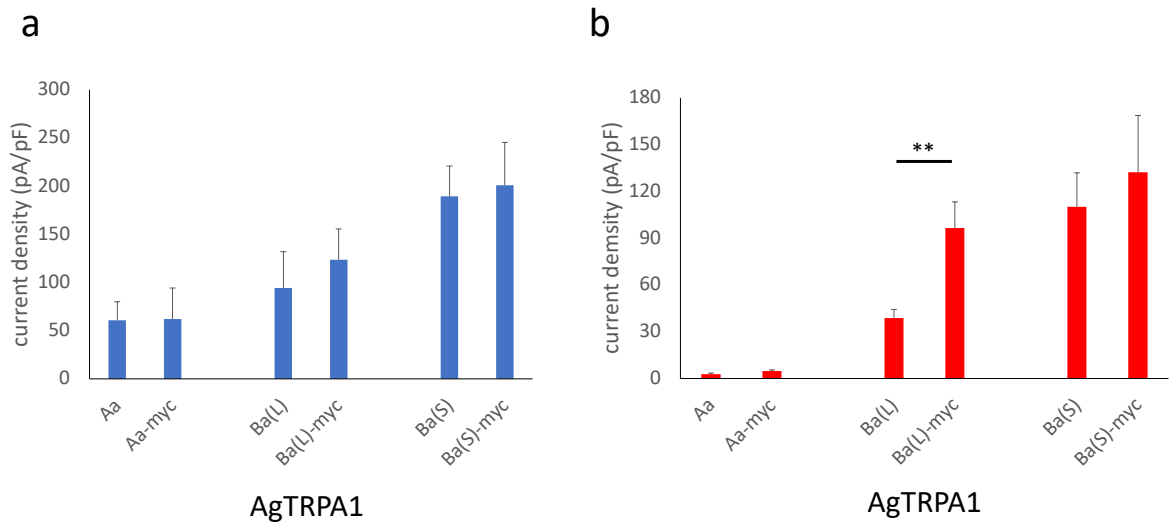

Figure 8.3 Effects of the Myc sequence in the N-terminus of AgTRPA1 on channel properties.

3 mM citronellal-evoked currents (a) and heat-induced currents (b) were recorded from naïve HEK293 cells expressing AgTRPA1Aa, AgTRPA1Ba(L) and AgTRPA1Ba(S) with or without Myc tags. All values are means ± S.E.M; $5 \leqslant n \leqslant 20$ each; **, $P < 0.01$.

3.9 Plasma membrane localization of AgTRPA1

AgTRPA1Ba(L) and AgTRPA1Ba(S) differ by 14 amino acid residues. Previous Western blotting results indicated that there might be a difference in the expression levels between these 2 channels on the plasma membrane. To investigate the membrane expression levels of different variants in detail, TRPA1-expressing HEK293 cells were biotinylated and the amounts of TRPA1 on plasma membrane were examined. Three Myc-tagged constructs of *AgTrpA1* plasmids were transfected into HEK293 cells and then heterologously-expressed plasma membrane proteins were conjugated with biotin. After biotin labelling, plasma membrane proteins of AgTRPA1 were pulled down with streptavidin-beads and immunoreacted with the primary antibodies against Myc. Both AgTRPA1Aa and AgTRPA1Ba(L) were confirmed to translocate to the plasma membrane to a similar degree (Fig. 9), which is consistent with the results of Western blotting for AgTRPA1 channels in the plasma membrane portion (Fig. 8.2). However, when the amounts of AgTRPA1Ba(L) and AgTRPA1Ba(S) on the plasma membrane were compared, AgTRPA1Ba(S) showed much higher expression level than AgTRPA1Ba(L) (Fig. 9). The protein samples of AgTRPA1 from the eluate of whole-cell lysates were examined with Western blotting as a control. Relative protein amounts for AgTRPA1Ba(S) in cell lysates were also larger than AgTRPA1Ba(L), suggesting that the difference in the expression on the plasma membrane resulted from the difference in protein expression in the cells. The difference was also observed in regular Western blotting analysis (Fig. 8.2), indicating the reliability of this result. Furthermore, the difference in the protein levels between AgTRPA1Ba(S) and AgTRPA1Ba(L) could explain the difference in the current densities between the 2 variants (Fig. 3) to some extent.

a

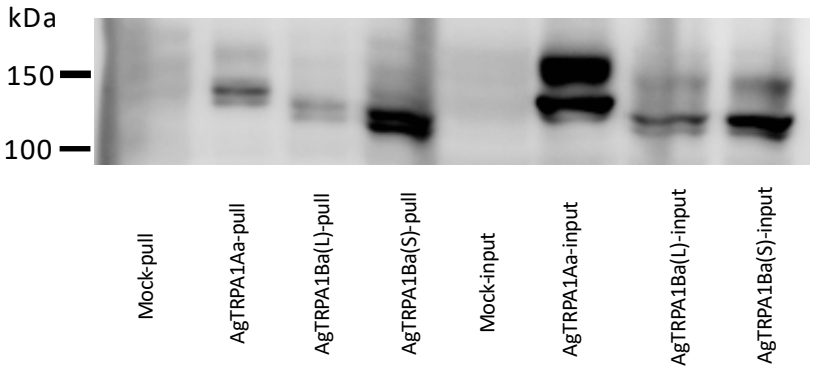

b

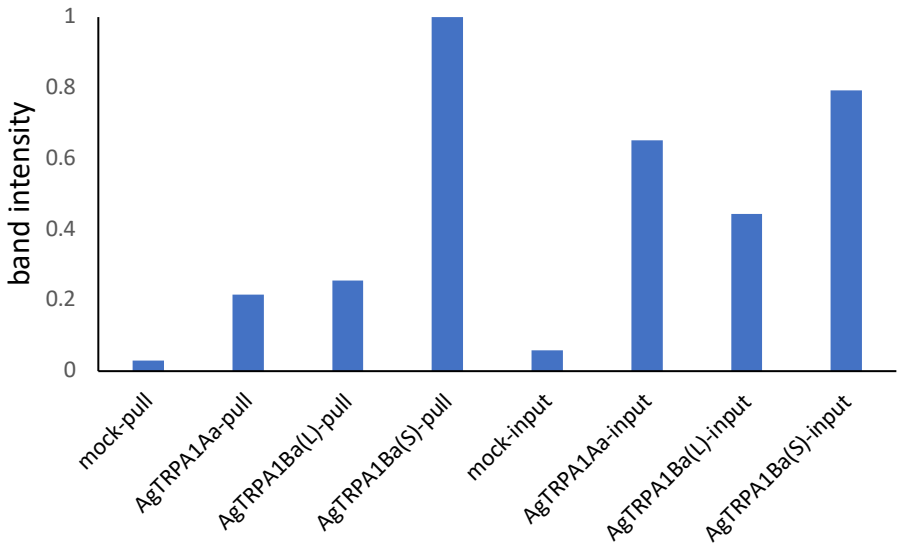

Figure 9 Quantification of the amounts of plasma membrane protein for AgTRPA1Aa, AgTRPA1Ba(L) and AgTRPA1Ba(S) in HEK293 cells. (a) The biotinylated membrane surface protein samples of AgTRPA1 (pull) were examined along with AgTRPA1 samples from the eluate of cell lysate (input). AgTRPA1 was detected with an antibody against Myc. (b) The amounts of AgTRPA1 proteins from the membrane surface and cell lysate were normalized to the AgTRPA1Ba(S)-pull sample.

3.10 Screening of potential mosquito repellents

TRPA1 is well-known to be activated by electrophilic compounds such as AITC and cinnamaldehyde. However, these conventional TRPA1 agonists are pungent compounds that irritate the skin, making them unappealing to most users. By quantifying the potencies of conventional TRPA1 agonists with a whole-cell patch-clamp method, I found that mosquito TRPA1 currents evoked by citronellal were comparable to those evoked by a strong electrophile, AITC (Fig. 7) as reported previously for citronellal for AgTRPA1 (Du et al., 2015). Therefore, I wondered if there were alternative compounds activating mosquito TRPA1, and I particularly focused on plant-derived compounds that are known to have anti-insect or anti-fungi efficacy.

Because screening with a whole-cell patch-clamp method is time-consuming, I screened those natural compounds described in section **2.7** with a fura-2 calcium-imaging method instead. Among 23 candidates examined, I found that octanal, nonanal and decanal potently activated AgTRPA1. These have been used commercially as components in perfumes and in flavor production for the food industry. Intriguingly, these 3 linear chain aldehydes have molecular structures similar to that of citronellal, and the difference is in the number of carbons in the main chain (Fig. 10.1). Fura-2 calcium-imaging experiments results are shown in APPENDIX 2. With regard to the other candidate mosquito repellents, carvacrol somehow increased intracellular calcium concentrations even in non-transfected HEK293 cells partly due to the high concentration (1 mM) used. Citral caused a slight increase in intracellular calcium concentrations. β-caryophyllene and diallyl disulfide increased intracellular calcium concentrations, too, although the increases were not as large as octanal, nonanal or decanal. Thus, I chose the 3 aldehydes for further analyses using a patch-clamp method. I also chose AgTRPA1Ba(S) for this analysis. I observed that large currents were activated by citronellal

through AgTRPA1Ba(S). Representative traces of the AgTRPA1Ba(S) currents activated by octanal, nonanal or decanal are shown in Figure 10.1. Interestingly, the channels were rapidly inactivated even in the presence of these compounds like in the citronellal-evoked currents (Fig. 10.1) possibly due to the desensitization after large activation.

The quantified results of whole-cell patch-clamp recordings indicated that these linear chain aldehydes activated AgTRPA1 in a dose-dependent manner, especially AgTRPA1Ba(S). Dose-dependent activation of AaTRPA1Ba(S) was also observed, although the current density was not as great as the ones with AgTRPA1Ba(S) (Fig. 10.2), suggesting these compounds could differently act on different mosquito species.

Figure 10 Octanal, nonanal and decanal are potential mosquito repellents.

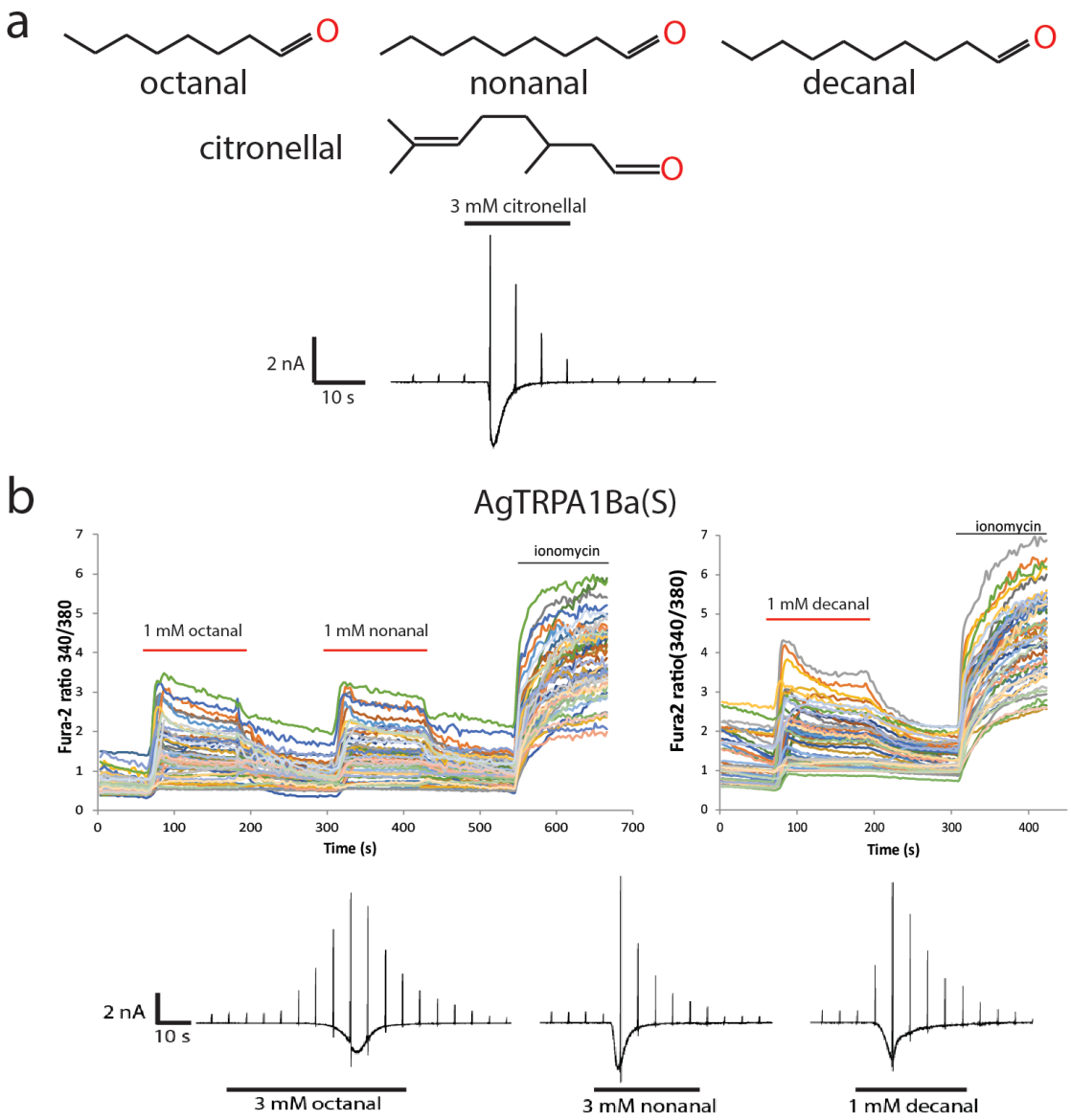

Figure 10.1 Molecular structures and representative AgTRPA1Ba(S) activating traces of octanal, nonanal and decanal. (a) Molecular formula of octanal, nonanal, decanal and citronellal. Representative traces of activation of AgTRPA1Ba(S) with 3 mM citronellal is shown. (b) Octanal, nonanal and decanal were screened for their capacities to activate AgTRPA1Ba(S) with both a fura-2 calcium-imaging method and a whole-cell patch-clamp method. Representative traces for AgTRPA1Ba(S) are shown.

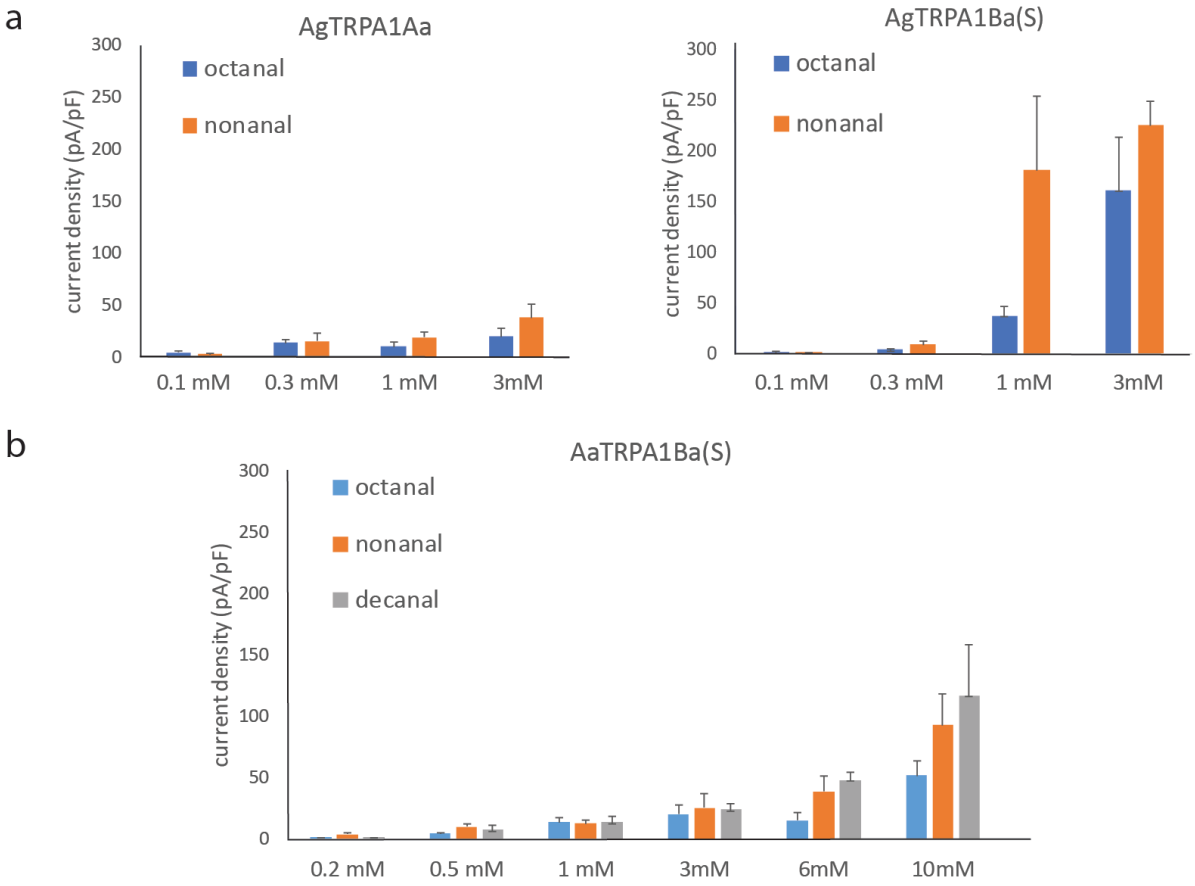

Figure 10.2 Effects of octanal, nonanal and decanal on AgTRPA1 and AaTRPA1

(a) Octanal and nonanal activated AgTRPA1 in a dose-dependent manner. (b) Octanal, nonanal and decanal activated AaTRPA1Ba(S) in a dose-dependent manner. All values are means ± S.E.M; $4 \leqslant n \leqslant 10$ each.

CHAPTER 4

Discussion

In this project, I acquired specimens of 3 important genera of mosquitoes. I planned to clone and identify multiple TRPA1 isoforms for a systematic comparison that has not yet been conducted. I was then involved in preliminary studies with newly identified TRPA1 variants to investigate whether these channels were sensitive to thermal or chemical stimuli. Further whole-cell patch-clamp studies indicated differences in both thermosensitivity and chemosensitivity among species. Distinct channel properties might result from different channel structures, and I found several critical determinants responsible for different TRPA1 channel properties. In addition, expression levels of mosquito TRPA1 on the cell membrane were examined to support my speculation regarding the underlying reasons for divergent channel properties. These discoveries should provide clues to help researchers better understand how mosquitoes evolved their sensory systems. Moreover, by characterizing the properties of mosquito TRPA1, development of specific agonists activating mosquito TRPA1 should be possible.

4.1 Molecular cloning of splicing variants of TRPA1 from disease vector mosquitoes

Previous research has utilized *Anopheles gambiae* as a model animal in which the AgTRPA1 channel was investigated (Hamada et al., 2008; Wang et al., 2009; Kang et al., 2010). In the light of discoveries of multiple splicing variants of *Drosophila melanogaster TrpA1* (Zhong et al., 2012; Kang et al., 2012), new research areas were opened for analysis because fruit flies and malaria mosquitoes are genetically close. Several splicing variants of *AgTrpA1* were recently discovered and have been characterized (Kang et al., 2012; Du et al., 2015). Using total RNA from 3 disease vector mosquito species, I performed molecular cloning. Different *TrpA1* transcripts of mosquitoes were cloned and sequenced. I also examined the genomic region of the same or closely related mosquito species in the vicinity of the *TrpA1* locus to

identify which exons encoded for these transcripts. Several highly conserved putative exons from *Anopheles stephensi*, *Aedes aegypti* and *Culex pipiens pallens* were determined. The amino acids encoded by different exons in the same region are barely aligned. Unlike the situation in which alternative splicing of the first 3 exons led to 2 different transcripts of *AgTrpA1* (Fig. 1.1 a), the N-terminal 97 amino acids are encoded by exons 1 and 2 for *AgTrpA1Aa* whereas the N-terminal 56 amino acids are encoded by exon 3 for *AgTrpA1Ba*. In the remaining 3 mosquito species, 2 additional alternatively spliced downstream exons were discovered. An exon (111 base pairs long) that encoded 37 amino acids was found in the transcripts of *AsTrpA1Ba*, *AaTrpA1Ba* and *CpTrpA1Ba*. Another exon (108 base pairs long) encoding 36 amino acids was implicated in the transcripts of *AsTrpA1Ab*, *AaTrpA1Ab*, *AaTrpA1Bb* and *CpTrpA1Ab* (Fig. 1.1 b-d). Theoretically, 4 distinct proteins are predicted from the combination of exons in these transcripts resembling the case of *Drosophila melanogaster TrpA1* (Zhong et al., 2012). The results of my cloning work showed that just 2 or 3 transcripts were detected from each species, and all the variants of *TrpA1A* have the 108-base pair long exon. Thus, they were named *TrpA1Ab*. It is unclear why there is only 1 unique *TrpA1Aa* instead of the ubiquitous *TrpA1Ab* in *Anopheles gambiae*.

4.2 The structural determinants that modulate mosquito TRPA1 channel properties

TRPA1 is activated by temperature changes as well as certain chemical compounds. Many regions of the TRPA1 channel contribute to its sensitivity to thermal or chemical stimuli. The critical determinants for TRPA1 modulation remain controversial. Electrophiles are known to activate most TRPA1 channels through covalent modification of cysteine residues in the ankyrin repeat domain (Hinman et al., 2006; Macpherson et al., 2007). The putative EF-hand between ankyrin repeat domains 11 and 12 was reported to be involved in intracellular

calcium-dependent activation of TRPA1 (Doerner et al. 2007; Zurborg et al. 2007). On the other hand, 3 negatively charged residues near the outer pore vestibule were found important for extracellular calcium-dependent heat-evoked activation in the green anole lizard TRPA1 (Kurganov et al., 2017).

In mosquito and fruit fly TRPA1s, different regions among the isoforms are located in the N-terminus and in the linker region between an ankyrin repeat domain and transmembrane domains, but no alternate amino acid changes were observed in the ankyrin repeat domain (Hamada et al., 2008). It was reported that the linker region is important for thermal sensation in *Drosophila melanogaster* TRPA1 (Zhong et al., 2012). While such comparisons can be conducted only in *Aedes aegypti*, I did not observe a significant difference in heat-evoked responses (Fig. 4), suggesting that the linker region is not critical for temperature sensitivity in mosquitoes. In order to examine the contribution of this linker domain to the heat-sensitivity in other mosquito TRPA1 proteins, chimeric channel studies are required. Here, I chose not to focus on the distinct linker regions in TRPA1 of *Anopheles stephensi* and *Culex pipiens pallens*. Therefore, the observed differences in channel properties are probably due to the varying length of the N-termini as reported in arthropods. Furthermore, the significantly different channel activities between TRPA1Ba(L) and TRPA1Ba(S) of *Anopheles gambiae* and *Aedes aegypti* may support my hypothesis that the N-terminus of TRPA1B is critical for modulating channel activity. TRPA1Ba(S) losing 14 amino acids showed large heat- and chemical-activated currents, again implying the N-terminal domain of mosquito TRPA1 is a crucial structural determinant.

4.3 Different thermosensitivities and chemosensitivities of TRPA1s among disease vector mosquitoes

4.3.1 The biogeoclimates of mosquito habitats confer distinct temperature-sensing properties to TRPA1B orthologues.

Functional diversity exists in thermosensitive TRP channels. TRPA1 orthologues were found to have distinct thermosensitivities in different species. Rodent TRPA1 was initially reported to be cold sensitive (Story et al., 2003) although some groups reported no temperature sensitivity of mouse TRPA1. In the case of human TRPA1, temperature sensitivity was not reported although there is a report showing that mutation in human TRPA1 causes pain sensation in a cold environment, suggesting the involvement of TRPA1 in cold-evoked events in some ways. Indeed, a group showed involvement of N-terminal proline hydration in TRPA1 sensitization in a cold environment. On the other hand, fruit fly TRPA1 was reported to be activated by warm temperatures (Saito and Tominaga, 2015). Even though these 4 mosquito species seem closely related, I readily observed differences in TRPA1 properties. First of all, when TRPA1A and TRPA1B were compared in the same species, TRPA1B showed larger heat responses than did TRPA1A (Fig. 5 a). This could be partly due to differences in the expression sites between TRPA1A and TRPA1B, as expression of the corresponding orthologues in *Drosophila* were reported to occur in the proboscis and elsewhere in the brain, respectively (Kang et al., 2012). Further, I summarized the temperature thresholds for heat stimulation of TRPA1B of each species and found that the TRPA1s of tropical mosquitoes (*Anopheles gambiae*, *Anopheles stephensi* and *Aedes aegypti*) had higher temperature thresholds (around 30^{o}C) than did *Culex pipiens pallens* (21.8^{o}C) mosquitoes that inhabit Nara prefecture with a cooler climate (Fig. 5 b). This difference suggests that *Culex pipiens pallens* has acclimated to a lower temperature so that it possesses a weaker thermal tolerance than the tropical mosquitoes. It is consistent with the observation that 30^{o}C is sufficient to adversely affect adult longevity, oviposition rates and egg hatch rates of *Culex pipiens pallens* (Oda et

al., 2002). The 21°C temperature is similar to that of silkworm TRPA1 and that determines their diapause phenotype (Sato et al., 2013). Coincidently, *Culex pipiens pallens* females also exhibit diapause, but *Culex pipiens quinquefasciatus* and *Culex pipiens molestus* inhabit warmer areas without diapause (Oda et al., 1987). It would be interesting to characterize the thermosensitivity of TRPA1 from the other 2 *Culex pipiens* species to elucidate the internal relation between TRPA1 and diapause.

4.3.2 Different evolutionary trajectories render divergent mechanisms for chemical sensation in mosquitoes.

Arthropods possess different repertoires of TRP channels compared to vertebrates (Saito and Tominaga, 2015). Arthropod species have the most diversified TRPA1 subfamily members because they exhibit extensive evolutionary plasticity (Kadowaki, 2015). The evolutionary origin of many disease vector mosquitoes was revealed in 2014, and *Anopheles gambiae* and *Anopheles stephensi* are closely related sister taxa that split 30.4 mya. On the other hand, *Aedes aegypti* and *Culex pipiens* are in a basal clade that diversified 56.9 mya. All these species share a common ancestor dated to 147.6 mya (Kamali et al., 2014). Each mosquito species studied in this project has at least 2 splicing variants of TRPA1. Two major differences could be found between these mosquito species from 2 clades. First, the multiple comparisons in section **3.7** indicated that there might be differences between these 2 clades in their abilities to sense chemicals. AaTRPA1 and CpTRPA1 were capable of detecting very low concentrations of AITC and citronellal while *Anopheles* TRPA1 could not. Second, TRPA1A of *Aedes aegypti* and *Culex pipiens pallens* were found to be more chemosensitive than TRPA1B, which is the opposite in *Anopheles* mosquitoes. The amino acid alignment of TRPA1 indicates that the critical conservative cysteine residues located in the ankyrin repeat domain are mostly

conserved in all the variants of the 4 mosquito species (APPENDIX 1). I speculate that there might be other important residues outside of the N-terminal region that play important roles in modulating and regulating chemical sensitivity.

4.4 TRPA1 expression in a heterologous expression system

In previous studies of insect TRPA1, investigators chose a *Xenopus* oocyte system for heterologous expression partly because lower temperature conditions were preferable for the ion channels from poikilothermic animals. In this project, I employed HEK293 cells to conduct whole-cell patch-clamp recordings.

When diverse current sizes are recorded from HEK293 cells, normally it is thought to be the consequence of different expression levels of variants of TRPA1. Nevertheless, if the difference between two channels is very slight, it is puzzling to have a significant difference in current size. Is a small current size due to a poor expression level? In section **3.8**, I measured the expression levels of Myc-tagged AgTRPA1Aa, AgTRPA1Ba(L) and AgTRPA1Ba(S). The channel properties of Myc-tagged AgTRPA1 and untagged ones were also compared. When I compared the expression levels of Myc-tagged AgTRPA1Aa and AgTRPA1Ba, it became clear that the negligible thermosensitivity of TRPA1Aa could not be explained by its expression on the cell membrane (Fig. 7.2 b & 7.3). When I compared the protein expression of AgTRPA1Ba(L) and AgTRPA1Ba(S), the situation became puzzling because the difference in current densities was parallel to the membrane expression levels. Therefore, I cannot rule out the possibility that the difference between longer and shorter TRPA1B results from different expression levels. Furthermore, I employed a straightforward method by which the 14-amino-acid-long peptide could be diffused inside HEK293 cells. Hence, the peptide overexpression condition could be simulated. Even high intracellular concentrations of such a peptide in HEK293 cells

did not alter the thermosensitivity of AgTRPA1Ba(S), suggesting that smaller currents evoked by heat in the cells expressing AgTRPA1Ba(L) were not caused by the binding of the 14 amino acids to the channel. Upon subsequently performing a biotinylating assay of plasma membrane protein, the expression level of AgTRPA1Ba(S) on the HEK293 cell membrane was much higher than that of AgTRPA1Ba(L). This would explain why both thermosensitivity and chemosensitivity of AgTRPA1Ba(L) were significantly lower. The mechanism by which 14 amino acids at the N-terminus of TRPA1 alter the expression level of TRPA1 on the plasma membrane remains to be clarified. I also compared Myc-tagged AgTRPA1 channels with untagged AgTRPA1 channels, and heat or a high concentration of citronellal was applied to generate a maximal current. No significant difference was found in citronellal-evoked currents, while the current density recorded from HEK293 cells transfected with an *AgTrpA1Ba(L)*-Myc-tagged plasmid was significantly larger. It is difficult to explain the cause of this phenomenon, but it highlights the importance of the TRPA1 N-terminus for thermal sensitivity.

4.5 Activation of TRPA1 channels by linear chain aldehydes

Development of novel effective mosquito repellents is crucial for controlling mosquito-borne diseases. Three linear chain aldehydes (octanal, nonanal and decanal) were found to potently activate AgTRPA1. Those aldehydes differ in the number of carbons in the main chain. The conventional mosquito TRPA1 agonist citronellal (3,7-dimethyloct-6-en-1-al) has 2 more methyl groups in the side chain and one more double bond in the main chain compared with octanal, the 8-carbon aldehyde. Aldehydes act as electrophiles to covalently modify cysteine residues within the ankyrin repeat domain to activate TRPA1 (Hinman et al., 2006; Macpherson et al., 2007). The sensitivity of TRPA1 to aldehydes might depend on the length

of the backbone because different current sizes were recorded in AgTRPA1Ba(S) in response to the same concentrations of octanal or nonanal (Fig. 8.2 a). The stability of the aldehydes in the lipid bilayers might play a role. Because the currents evoked by these aldehydes were smaller in AaTRPA1Ba(S) than in AgTRPA1Ba(S), it would be worth measuring the effects of these chemicals on AaTRPA1Ab since the subsequent characterization of TRPA1 indicated that AaTRPA1Ab is more sensitive. I also tested octanoic acid, nonanoic acid and decanoic acid in which the formyl group of the corresponding aldehydes is substituted with a carboxyl group. However, no appreciable changes in intracellular calcium concentrations were detected (APPENDIX 2). On the other hand, the aforementioned fatty acids were reported to activate human TRPA1 and fire ant TRPA (Terada et al., 2011; Wang et al., 2018). These facts suggest species-specific modulation of TRPA1 orthologues for detecting noxious stimuli.

4.6 Limitations of the work to date and future perspectives

Convincing data were obtained in this study by conducting whole-cell patch-clamp experiments with heterologously expressed mosquito TRPA1. However, I had only one opportunity to perform an experiment with a potential repellent *in vivo* (data not shown). For behavioral experiments investigating the differences of thermosensitivity and chemosensitivity among mosquito species, no progress has been made so far. Therefore, further behavioral analyses are absolutely necessary to support my *in vitro* data. In addition, although Western blotting and biotinylation experiments have been performed to determine the expression level of TRPA1 on the cell membrane, the mechanisms by which these amino acids affect protein expression on the membrane remain mysterious.

4.7 Conclusions

In this project, I successfully cloned multiple splicing variants of TRPA1 from disease vector mosquitoes including *Anopheles stephensi*, *Aedes aegypti* and *Culex pipiens pallens.* TRPA1 splicing variants had not been studied across different mosquito species prior to this investigation. I discovered here that there are an extra 14 amino acids in the N-termini of AgTRPA1B and AaTRPA1B. I also employed a whole-cell patch-clamp method to investigate which part of the channel modulates its properties. I found that the thermosensitivity of TRPA1 reflects the thermal tolerance for the climate in which each species lives. In addition, I demonstrated that different TRPA1 expression levels on the cell membrane do not explain the divergent channel properties. Finally, I undertook the screening of potential mosquito repellents from plant-derived chemical compounds using fura-2 calcium-imaging. Three linear chain aldehydes structurally similar to citronellal were found to be novel mosquito TRPA1 agonists. In the future, the results of this project could be extended using mosquitoes for behavioral analysis to unravel the mechanism by which TRPA1 functions in the regulation of mosquito host-seeking and avoidance behaviors.

References

1 Bautista, D. M. *et al.* TRPA1 mediates the inflammatory actions of environmental irritants and proalgesic agents. *Cell* **124**, 1269-1282, doi:10.1016/j.cell.2006.02.023 (2006).

2 Cai, X. Unicellular Ca2+ signaling 'toolkit' at the origin of metazoa. *Mol Biol Evol* **25**, 1357-1361, doi:10.1093/molbev/msn077 (2008).

3 Caterina, M. J. *et al.* The capsaicin receptor: a heat-activated ion channel in the pain pathway. *Nature* **389**, 816-824, doi:10.1038/39807 (1997).

4 Cordero-Morales, J., Gracheva, E. & Julius, D. *Cytoplasmic Ankyrin Repeats of Transient Receptor Potential A1 (TRPA1) Dictate Sensitivity to Thermal and Chemical Stimuli*. Vol. 108 (2011).

5 Corfas, R. A. & Vosshall, L. B. The cation channel TRPA1 tunes mosquito thermotaxis to host temperatures. *Elife* **4**, doi:10.7554/eLife.11750 (2015).

6 Dash, A., Adak, T., Kamaraju, R. & Singh, O. *The biology and control of malaria vectors in India*. Vol. 92 (2007).

7 Dekker, T., Geier, M. & Carde, R. T. Carbon dioxide instantly sensitizes female yellow fever mosquitoes to human skin odours. *J Exp Biol* **208**, 2963-2972, doi:10.1242/jeb.01736 (2005).

8 Doerner, J. F., Gisselmann, G., Hatt, H. & Wetzel, C. H. Transient receptor potential channel A1 is directly gated by calcium ions. *J Biol Chem* **282**, 13180-13189, doi:10.1074/jbc.M607849200 (2007).

9 Du, E. J. *et al.* The Mosquito Repellent Citronellal Directly Potentiates Drosophila TRPA1, Facilitating Feeding Suppression. *Mol Cells* **38**, 911-917, doi:10.14348/molcells.2015.0215 (2015).

10 Dunham, J. P., Kelly, S. & Donaldson, L. F. Inflammation reduces mechanical thresholds in a population of transient receptor potential channel A1-expressing nociceptors in the rat. *Eur J Neurosci* **27**, 3151-3160, doi:10.1111/j.1460-9568.2008.06256.x (2008).

11 E. Davis, E. & G. Sokolove, P. *Temperature responses of antennal receptors of the mosquito, Aedes aegypti*. Vol. 96 (1975).

12 Eiras, A. E. & Jepson, P. C. Responses of female Aedes aegypti (Diptera: Culicidae) to host odours and convection currents using an olfactometer bioassay. *Bulletin of Entomological Research* **84**, 207, doi:10.1017/s0007485300039705 (2009).

13 Hamada, F. N. *et al.* An internal thermal sensor controlling temperature preference in Drosophila. *Nature* **454**, 217-220, doi:10.1038/nature07001 (2008).

14 Hinman, A., Chuang, H. H., Bautista, D. M. & Julius, D. TRP channel activation by reversible covalent modification. *Proc Natl Acad Sci U S A* **103**, 19564-19568, doi:10.1073/pnas.0609598103 (2006).

15 Inocente, E. A., Shaya, M., Acosta, N., Rakotondraibe, L. H. & Piermarini, P. M. A natural agonist of mosquito TRPA1 from the medicinal plant Cinnamosma fragrans that is toxic, antifeedant, and repellent to the yellow fever mosquito Aedes aegypti. *PLoS Negl Trop Dis* **12**, e0006265, doi:10.1371/journal.pntd.0006265 (2018).

16 Jordt, S. E. *et al.* Mustard oils and cannabinoids excite sensory nerve fibres through the TRP channel ANKTM1. *Nature* **427**, 260-265, doi:10.1038/nature02282 (2004).

17 Kadowaki, T. Evolutionary dynamics of metazoan TRP channels. *Pflugers Arch* **467**, 2043-2053, doi:10.1007/s00424-015-1705-5 (2015).

18 Kamali, M. *et al.* Multigene phylogenetics reveals temporal diversification of major African malaria vectors. *PLoS One* **9**, e93580, doi:10.1371/journal.pone.0093580 (2014).

19 Kang, K. *et al.* Modulation of TRPA1 thermal sensitivity enables sensory discrimination in Drosophila. *Nature* **481**, 76-80, doi:10.1038/nature10715 (2011).

20 Kang, K. *et al.* Analysis of Drosophila TRPA1 reveals an ancient origin for human chemical nociception. *Nature* **464**, 597-600, doi:10.1038/nature08848 (2010).

21 Kremeyer, B. *et al.* A gain-of-function mutation in TRPA1 causes familial episodic pain syndrome. *Neuron* **66**, 671-680, doi:10.1016/j.neuron.2010.04.030 (2010).

22 Kwan, K. Y. & Corey, D. P. Burning cold: involvement of TRPA1 in noxious cold sensation. *J Gen Physiol* **133**, 251-256, doi:10.1085/jgp.200810146 (2009).

23 Lacey, E. S., Ray, A. & Carde, R. T. Close encounters: contributions of carbon dioxide and human skin odour to finding and landing on a host in Aedes aegypti. *Physiol Entomol* **39**, 60-68, doi:10.1111/phen.12048 (2014).

24 Leake, C. The biology of mosquitoes. Volume 1: Development, nutrition and reproduction. *Transactions of the Royal Society of Tropical Medicine and Hygiene* **87**, 718, doi:10.1016/0035-9203(93)90329-O (1993).

25 Lee, Y. *et al.* Pyrexia is a new thermal transient receptor potential channel endowing tolerance to high temperatures in Drosophila melanogaster. *Nat Genet* **37**, 305-310, doi:10.1038/ng1513 (2005).

26 Luo, J., Shen, W. L. & Montell, C. TRPA1 mediates sensation of the rate of temperature change in Drosophila larvae. *Nat Neurosci* **20**, 34-41, doi:10.1038/nn.4416 (2017).

27 Macpherson, L. J. *et al.* Noxious compounds activate TRPA1 ion channels through covalent modification of cysteines. *Nature* **445**, 541-545, doi:10.1038/nature05544 (2007).

28 Majikina, A., Takahashi, K., Saito, S., Tominaga, M. & Ohta, T. Involvement of nociceptive transient receptor potential channels in repellent action of pulegone.

Biochem Pharmacol **151**, 89-95, doi:10.1016/j.bcp.2018.02.032 (2018).

29 Matsuura, H., Sokabe, T., Kohno, K., Tominaga, M. & Kadowaki, T. Evolutionary conservation and changes in insect TRP channels. *BMC Evol Biol* **9**, 228, doi:10.1186/1471-2148-9-228 (2009).

30 Miyake, T. *et al.* Cold sensitivity of TRPA1 is unveiled by the prolyl hydroxylation blockade-induced sensitization to ROS. *Nat Commun* **7**, 12840, doi:10.1038/ncomms12840 (2016).

31 Mogi, M. The forms of the Culex pipiens complex in East Asia, with ecological thoughts on their origin and interrelation. *J Am Mosq Control Assoc* **28**, 28-52, doi:10.2987/8756-971X-28.4s.28 (2012).

32 Montell, C. & Rubin, G. M. Molecular characterization of the Drosophila trp locus: a putative integral membrane protein required for phototransduction. *Neuron* **2**, 1313-1323 (1989).

33 Neely, G. G. *et al.* TrpA1 regulates thermal nociception in Drosophila. *PLoS One* **6**, e24343, doi:10.1371/journal.pone.0024343 (2011).

34 Oda, T. *et al.* Reproductive Activity and Survival ofCulex pipiens pallensandCulex quinquefasciatus(Diptera: Culicidae) in Japan at High Temperature. *Journal of Medical Entomology* **39**, 185-190, doi:10.1603/0022-2585-39.1.185 (2002).

35 Oda, T. *et al. Studies on Imaginal Diapause in Culex pipiens Complex in Japan*. Vol. 1 (1987).

36 Oliva, C., Cohen, I. S. & Mathias, R. T. Calculation of time constants for intracellular diffusion in whole cell patch clamp configuration. *Biophysical journal* **54**, 791-799, doi:10.1016/s0006-3495(88)83017-0 (1988).

37 Omondi, B. A., Majeed, S. & Ignell, R. Functional development of carbon dioxide

detection in the maxillary palp of Anopheles gambiae. *J Exp Biol* **218**, 2482-2488, doi:10.1242/jeb.116798 (2015).

38 Paulsen, C. E., Armache, J. P., Gao, Y., Cheng, Y. & Julius, D. Structure of the TRPA1 ion channel suggests regulatory mechanisms. *Nature* **520**, 511-517, doi:10.1038/nature14367 (2015).

39 Peng, G. *et al.* Plant-Derived Tick Repellents Activate the Honey Bee Ectoparasitic Mite TRPA1. *Cell Rep* **12**, 190-202, doi:10.1016/j.celrep.2015.06.025 (2015).

40 Peng, G., Shi, X. & Kadowaki, T. Evolution of TRP channels inferred by their classification in diverse animal species. *Mol Phylogenet Evol* **84**, 145-157, doi:10.1016/j.ympev.2014.06.016 (2015).

41 Rosenzweig, M. *et al.* The Drosophila ortholog of vertebrate TRPA1 regulates thermotaxis. *Genes Dev* **19**, 419-424, doi:10.1101/gad.1278205 (2005).

42 S., K. J. The Visual Responses of Flying Mosquitoes. *Proceedings of the Zoological Society of London* **A109**, 221-242, doi:doi:10.1111/j.1096-3642.1940.tb00831.x (1940).

43 Saito, S. *et al.* Analysis of transient receptor potential ankyrin 1 (TRPA1) in frogs and lizards illuminates both nociceptive heat and chemical sensitivities and coexpression with TRP vanilloid 1 (TRPV1) in ancestral vertebrates. *J Biol Chem* **287**, 30743-30754, doi:10.1074/jbc.M112.362194 (2012).

44 Saito, S. & Tominaga, M. Functional diversity and evolutionary dynamics of thermoTRP channels. *Cell Calcium* **57**, 214-221, doi:10.1016/j.ceca.2014.12.001 (2015).

45 Sato, A. *et al.* Embryonic thermosensitive TRPA1 determines transgenerational diapause phenotype of the silkworm, Bombyx mori. *Proc Natl Acad Sci U S A* **111**, E1249-1255, doi:10.1073/pnas.1322134111 (2014).

46 Story, G. M. *et al.* ANKTM1, a TRP-like channel expressed in nociceptive neurons, is

activated by cold temperatures. *Cell* **112**, 819-829 (2003).

47 Survery, S. *et al.* The N-terminal Ankyrin Repeat Domain Is Not Required for Electrophile and Heat Activation of the Purified Mosquito TRPA1 Receptor. *J Biol Chem* **291**, 26899-26912, doi:10.1074/jbc.M116.743443 (2016).

48 Terada, Y., Narukawa, M. & Watanabe, T. Specific hydroxy fatty acids in royal jelly activate TRPA1. *J Agric Food Chem* **59**, 2627-2635, doi:10.1021/jf1041646 (2011).

49 Tominaga, M. *et al.* The cloned capsaicin receptor integrates multiple pain-producing stimuli. *Neuron* **21**, 531-543 (1998).

50 Tracey, W. D., Jr., Wilson, R. I., Laurent, G. & Benzer, S. painless, a Drosophila gene essential for nociception. *Cell* **113**, 261-273 (2003).

51 van Breugel, F., Riffell, J., Fairhall, A. & Dickinson, M. H. Mosquitoes Use Vision to Associate Odor Plumes with Thermal Targets. *Curr Biol* **25**, 2123-2129, doi:10.1016/j.cub.2015.06.046 (2015).

52 Viswanath, V. *et al.* Opposite thermosensor in fruitfly and mouse. *Nature* **423**, 822-823, doi:10.1038/423822a (2003).

53 Wang, G. *et al.* Anopheles gambiae TRPA1 is a heat-activated channel expressed in thermosensitive sensilla of female antennae. *Eur J Neurosci* **30**, 967-974, doi:10.1111/j.1460-9568.2009.06901.x (2009).

54 Wang, X. *et al.* HsTRPA of the Red Imported Fire Ant, Solenopsis invicta, Functions as a Nocisensor and Uncovers the Evolutionary Plasticity of HsTRPA Channels. *eNeuro* **5**, doi:10.1523/ENEURO.0327-17.2018 (2018).

55 Zayats, V. *et al.* Regulation of the transient receptor potential channel TRPA1 by its N-terminal ankyrin repeat domain. *Journal of molecular modeling* **19**, 4689-4700, doi:10.1007/s00894-012-1505-1 (2013).

56 Zhong, L. *et al.* Thermosensory and nonthermosensory isoforms of Drosophila melanogaster TRPA1 reveal heat-sensor domains of a thermoTRP Channel. *Cell Rep* **1**, 43-55, doi:10.1016/j.celrep.2011.11.002 (2012).

57 Zhou, Y., Suzuki, Y., Uchida, K. & Tominaga, M. Identification of a splice variant of mouse TRPA1 that regulates TRPA1 activity. *Nat Commun* **4**, 2399, doi:10.1038/ncomms3399 (2013).

58 Zurborg, S., Yurgionas, B., Jira, J. A., Caspani, O. & Heppenstall, P. A. Direct activation of the ion channel TRPA1 by Ca2+. *Nat Neurosci* **10**, 277-279, doi:10.1038/nn1843 (2007).

a

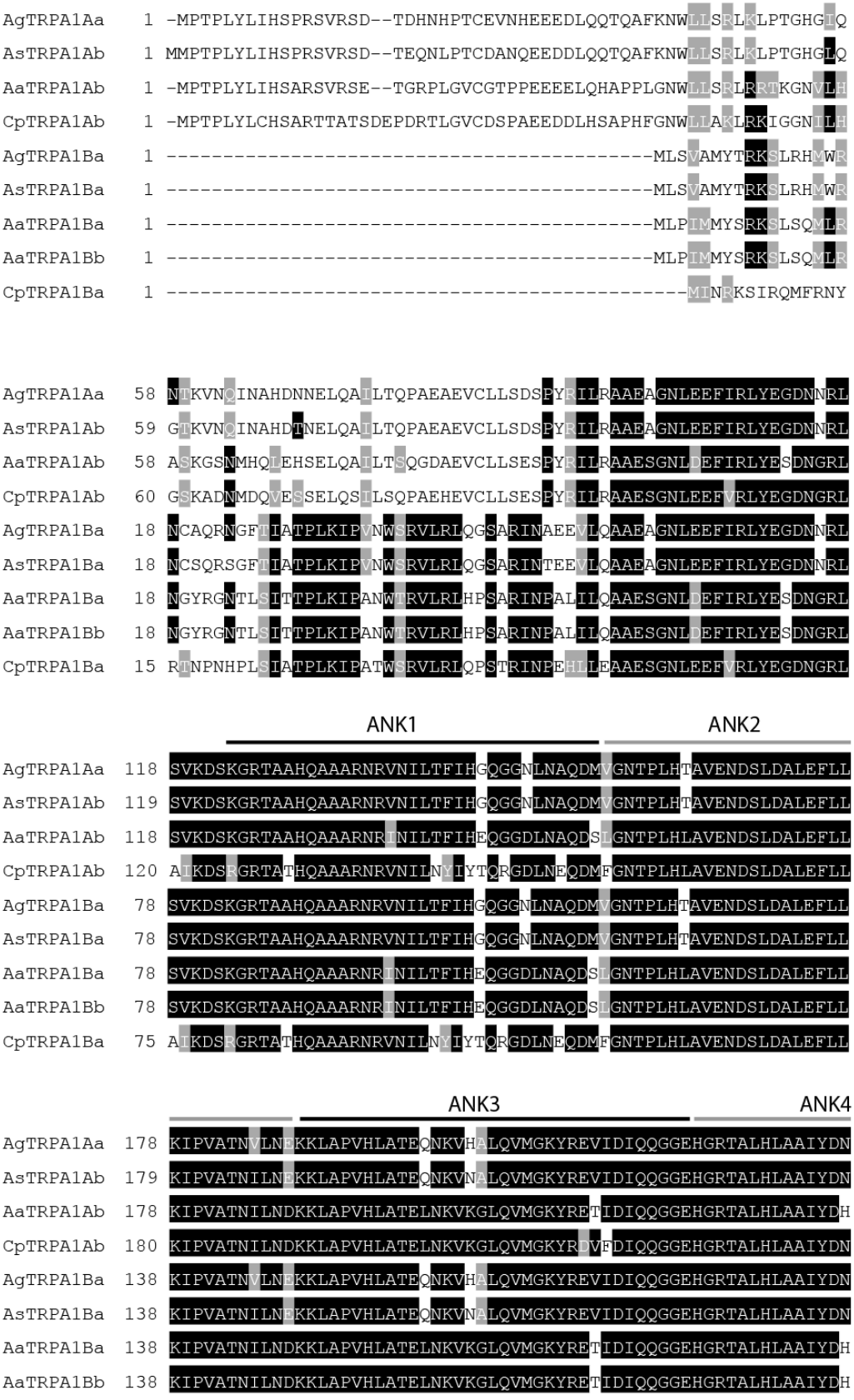
AgTRPA1Aa
AsTRPA1Ab
AaTRPA1Ab
CpTRPA1Ab
AgTRPA1Ba
AsTRPA1Ba
AaTRPA1Ba
AaTRPA1Bb
CpTRPA1Ba
ANK1
ANK2
ANK3
ANK4

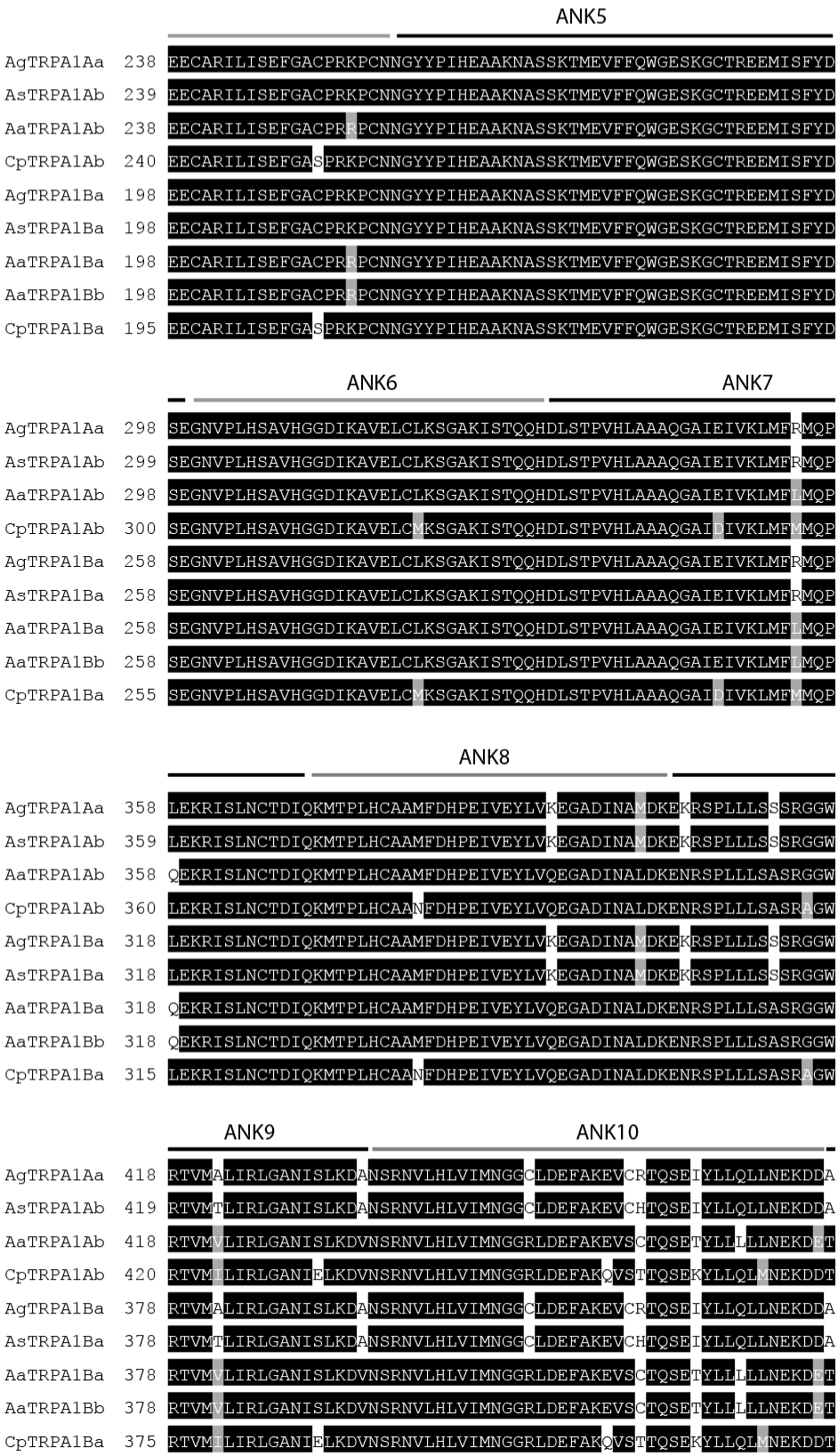
ANK5
AgTRPA1Aa 238 EECARILISEFGACPRKPCNNGYYPIHEAAKNASSKTMEVFFQWGESKGCTREEMISFYD
AsTRPA1Ab 239 EECARILISEFGACPRKPCNNGYYPIHEAAKNASSKTMEVFFQWGESKGCTREEMISFYD
AaTRPA1Ab 238 EECARILISEFGACPRRPCNNGYYPIHEAAKNASSKTMEVFFQWGESKGCTREEMISFYD
CpTRPA1Ab 240 EECARILISEFGASPRKPCNNGYYPIHEAAKNASSKTMEVFFQWGESKGCTREEMISFYD
AgTRPA1Ba 198 EECARILISEFGACPRKPCNNGYYPIHEAAKNASSKTMEVFFQWGESKGCTREEMISFYD
AsTRPA1Ba 198 EECARILISEFGACPRKPCNNGYYPIHEAAKNASSKTMEVFFQWGESKGCTREEMISFYD
AaTRPA1Ba 198 EECARILISEFGACPRRPCNNGYYPIHEAAKNASSKTMEVFFQWGESKGCTREEMISFYD
AaTRPA1Bb 198 EECARILISEFGACPRRPCNNGYYPIHEAAKNASSKTMEVFFQWGESKGCTREEMISFYD
CpTRPA1Ba 195 EECARILISEFGASPRKPCNNGYYPIHEAAKNASSKTMEVFFQWGESKGCTREEMISFYD
ANK6
ANK7
AgTRPA1Aa 298 SEGNVPLHSAVHGGDIKAVELCLKSGAKISTQQHDLSTPVHLAAAQGAIEIVKLMFRMQP
AsTRPA1Ab 299 SEGNVPLHSAVHGGDIKAVELCLKSGAKISTQQHDLSTPVHLAAAQGAIEIVKLMFRMQP
AaTRPA1Ab 298 SEGNVPLHSAVHGGDIKAVELCLKSGAKISTQQHDLSTPVHLAAAQGAIEIVKLMFIMQP
CpTRPA1Ab 300 SEGNVPLHSAVHGGDIKAVELCMKSGAKISTQQHDLSTPVHLAAAQGAIDIVKLMFVMQP
AgTRPA1Ba 258 SEGNVPLHSAVHGGDIKAVELCLKSGAKISTQQHDLSTPVHLAAAQGAIEIVKLMFRMQP
AsTRPA1Ba 258 SEGNVPLHSAVHGGDIKAVELCLKSGAKISTQQHDLSTPVHLAAAQGAIEIVKLMFRMQP
AaTRPA1Ba 258 SEGNVPLHSAVHGGDIKAVELCLKSGAKISTQQHDLSTPVHLAAAQGAIEIVKLMFIMQP
AaTRPA1Bb 258 SEGNVPLHSAVHGGDIKAVELCLKSGAKISTQQHDLSTPVHLAAAQGAIEIVKLMFIMQP
CpTRPA1Ba 255 SEGNVPLHSAVHGGDIKAVELCMKSGAKISTQQHDLSTPVHLAAAQGAIDIVKLMFVMQP
ANK8
AgTRPA1Aa 358 LEKRISLNCTDIQKMTPLHCAAMFDHPEIVEYLVKEGADINAMDKEKRSPLLLSSSRGGW
AsTRPA1Ab 359 LEKRISLNCTDIQKMTPLHCAAMFDHPEIVEYLVKEGADINAMDKEKRSPLLLSSSRGGW
AaTRPA1Ab 358 QEKRISLNCTDIQKMTPLHCAAMFDHPEIVEYLVQEGADINALDKENRSPLLLSASRGGW
CpTRPA1Ab 360 LEKRISLNCTDIQKMTPLHCAANFDHPEIVEYLVQEGADINALDKENRSPLLLSASRAGW
AgTRPA1Ba 318 LEKRISLNCTDIQKMTPLHCAAMFDHPEIVEYLVKEGADINAMDKEKRSPLLLSSSRGGW
AsTRPA1Ba 318 LEKRISLNCTDIQKMTPLHCAAMFDHPEIVEYLVKEGADINAMDKEKRSPLLLSSSRGGW
AaTRPA1Ba 318 QEKRISLNCTDIQKMTPLHCAAMFDHPEIVEYLVQEGADINALDKENRSPLLLSASRGGW
AaTRPA1Bb 318 QEKRISLNCTDIQKMTPLHCAAMFDHPEIVEYLVQEGADINALDKENRSPLLLSASRGGW
CpTRPA1Ba 315 LEKRISLNCTDIQKMTPLHCAANFDHPEIVEYLVQEGADINALDKENRSPLLLSASRAGW
ANK9
ANK10
AgTRPA1Aa 418 RTVMALIRLGANISLKDANSRNVLHLVIMNGGCLDEFAKEVCRTQSEIYLLQLLNEKDDA
AsTRPA1Ab 419 RTVMTLIRLGANISLKDANSRNVLHLVIMNGGCLDEFAKEVCHTQSEIYLLQLLNEKDDA
AaTRPA1Ab 418 RTVMVLIRLGANISLKDVNSRNVLHLVIMNGGRLDEFAKEVSCTQSETYLLLLNEKDET
CpTRPA1Ab 420 RTVMILIRLGANIELKDVNSRNVLHLVIMNGGRLDEFAKQVSTTQSEKYLLQLMNEKDDT
AgTRPA1Ba 378 RTVMALIRLGANISLKDANSRNVLHLVIMNGGCLDEFAKEVCRTQSEIYLLQLLNEKDDA
AsTRPA1Ba 378 RTVMTLIRLGANISLKDANSRNVLHLVIMNGGCLDEFAKEVCHTQSEIYLLQLLNEKDDA
AaTRPA1Ba 378 RTVMVLIRLGANISLKDVNSRNVLHLVIMNGGRLDEFAKEVSCTQSETYLLLLNEKDET
AaTRPA1Bb 378 RTVMVLIRLGANISLKDVNSRNVLHLVIMNGGRLDEFAKEVSCTQSETYLLLLNEKDET
CpTRPA1Ba 375 RTVMILIRLGANIELKDVNSRNVLHLVIMNGGRLDEFAKQVSTTQSEKYLLQLMNEKDDT

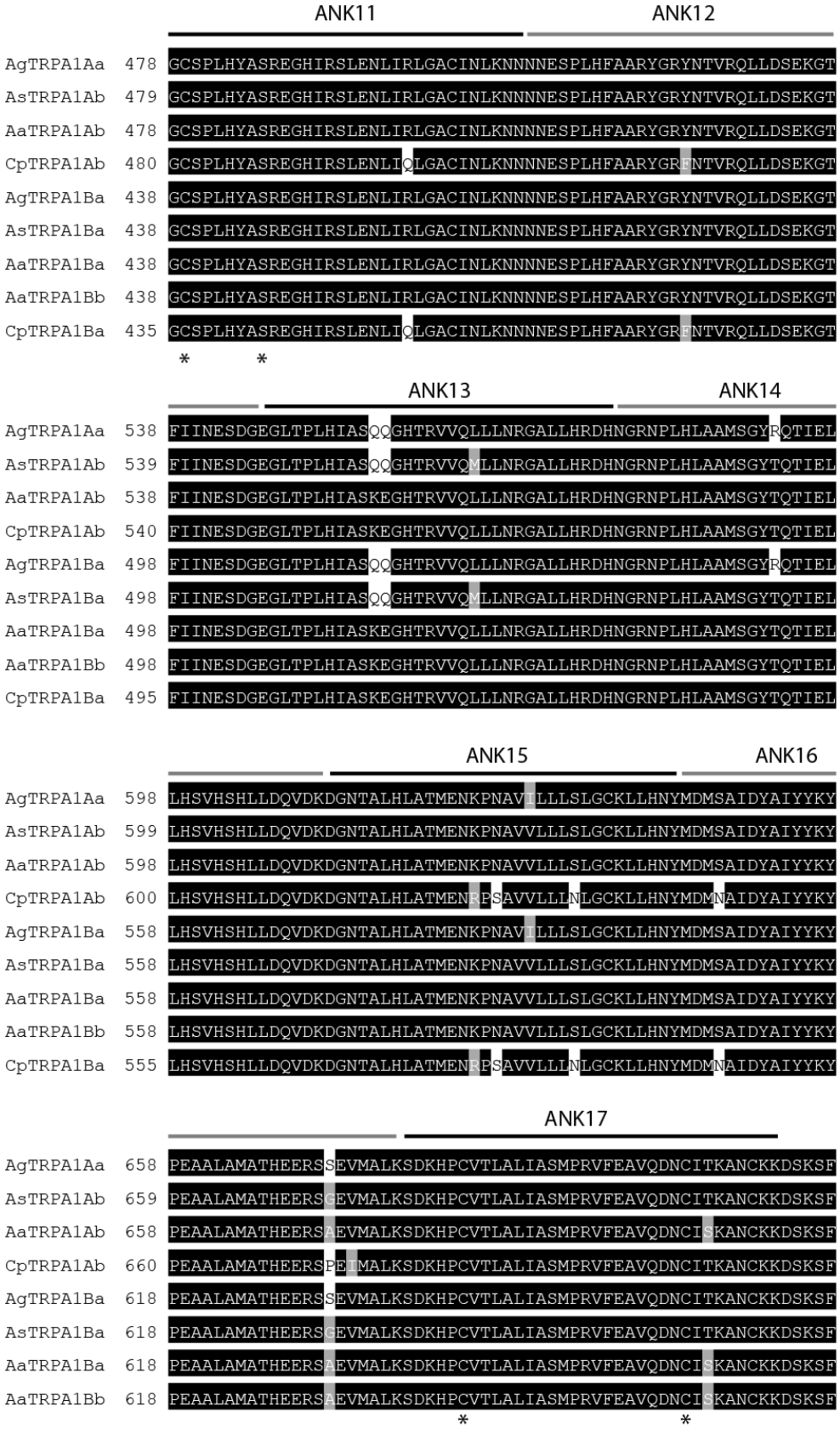
ANK11
ANK12
AgTRPA1Aa 478 GCSPLHYASREGHIRSLENLIRLGACINLKNNNNESPLHFAARYGRYNTVRQLLDSEKGT
AsTRPA1Ab 479 GCSPLHYASREGHIRSLENLIRLGACINLKNNNNESPLHFAARYGRYNTVRQLLDSEKGT
AaTRPA1Ab 478 GCSPLHYASREGHIRSLENLIRLGACINLKNNNNESPLHFAARYGRYNTVRQLLDSEKGT
CpTRPA1Ab 480 GCSPLHYASREGHIRSLENLIQLGACINLKNNNNESPLHFAARYGRFNTVRQLLDSEKGT
AgTRPA1Ba 438 GCSPLHYASREGHIRSLENLIRLGACINLKNNNNESPLHFAARYGRYNTVRQLLDSEKGT
AsTRPA1Ba 438 GCSPLHYASREGHIRSLENLIRLGACINLKNNNNESPLHFAARYGRYNTVRQLLDSEKGT
AaTRPA1Ba 438 GCSPLHYASREGHIRSLENLIRLGACINLKNNNNESPLHFAARYGRYNTVRQLLDSEKGT
AaTRPA1Bb 438 GCSPLHYASREGHIRSLENLIRLGACINLKNNNNESPLHFAARYGRYNTVRQLLDSEKGT
CpTRPA1Ba 435 GCSPLHYASREGHIRSLENLIQLGACINLKNNNNESPLHFAARYGRFNTVRQLLDSEKGT
* *
ANK13
ANK14
AgTRPA1Aa 538 FIINESDGEGLTPLHIASQQGHTRVVQLLLNRGALLHRDHNGRNPLHLAAMSGYRQTIEL
AsTRPA1Ab 539 FIINESDGEGLTPLHIASQQGHTRVVQMLLNRGALLHRDHNGRNPLHLAAMSGYTQTIEL
AaTRPA1Ab 538 FIINESDGEGLTPLHIASKEGHTRVVQLLLNRGALLHRDHNGRNPLHLAAMSGYTQTIEL
CpTRPA1Ab 540 FIINESDGEGLTPLHIASKEGHTRVVQLLLNRGALLHRDHNGRNPLHLAAMSGYTQTIEL
AgTRPA1Ba 498 FIINESDGEGLTPLHIASQQGHTRVVQLLLNRGALLHRDHNGRNPLHLAAMSGYRQTIEL
AsTRPA1Ba 498 FIINESDGEGLTPLHIASQQGHTRVVQMLLNRGALLHRDHNGRNPLHLAAMSGYTQTIEL
AaTRPA1Ba 498 FIINESDGEGLTPLHIASKEGHTRVVQLLLNRGALLHRDHNGRNPLHLAAMSGYTQTIEL
AaTRPA1Bb 498 FIINESDGEGLTPLHIASKEGHTRVVQLLLNRGALLHRDHNGRNPLHLAAMSGYTQTIEL
CpTRPA1Ba 495 FIINESDGEGLTPLHIASKEGHTRVVQLLLNRGALLHRDHNGRNPLHLAAMSGYTQTIEL
ANK15
ANK16
AgTRPA1Aa 598 LHSVHSHLLDQVDKDGNTALHLATMENKPNAVTLLLSLGCKLLHNYMDMSAIDYAIYYKY
AsTRPA1Ab 599 LHSVHSHLLDQVDKDGNTALHLATMENKPNAVVLLLSLGCKLLHNYMDMSAIDYAIYYKY
AaTRPA1Ab 598 LHSVHSHLLDQVDKDGNTALHLATMENKPNAVVLLLSLGCKLLHNYMDMSAIDYAIYYKY
CpTRPA1Ab 600 LHSVHSHLLDQVDKDGNTALHLATMENRPSAVVLLLNLGCKLLHNYMDMNAIDYAIYYKY
AgTRPA1Ba 558 LHSVHSHLLDQVDKDGNTALHLATMENKPNAVTLLLSLGCKLLHNYMDMSAIDYAIYYKY
AsTRPA1Ba 558 LHSVHSHLLDQVDKDGNTALHLATMENKPNAVVLLLSLGCKLLHNYMDMSAIDYAIYYKY
AaTRPA1Ba 558 LHSVHSHLLDQVDKDGNTALHLATMENKPNAVVLLLSLGCKLLHNYMDMSAIDYAIYYKY
AaTRPA1Bb 558 LHSVHSHLLDQVDKDGNTALHLATMENKPNAVVLLLSLGCKLLHNYMDMSAIDYAIYYKY
CpTRPA1Ba 555 LHSVHSHLLDQVDKDGNTALHLATMENRPSAVVLLLNLGCKLLHNYMDMNAIDYAIYYKY
ANK17
AgTRPA1Aa 658 PEAALAMATHEERSSEVMALKSDKHPCVTLALIASMPRVFEAVQDNCITKANCKKDSKSF
AsTRPA1Ab 659 PEAALAMATHEERSGEVMALKSDKHPCVTLALIASMPRVFEAVQDNCITKANCKKDSKSF
AaTRPA1Ab 658 PEAALAMATHEERSAEVMALKSDKHPCVTLALIASMPRVFEAVQDNCISKANCKKDSKSF
CpTRPA1Ab 660 PEAALAMATHEERSPEIMALKSDKHPCVTLALIASMPRVFEAVQDNCITKANCKKDSKSF
AgTRPA1Ba 618 PEAALAMATHEERSSEVMALKSDKHPCVTLALIASMPRVFEAVQDNCITKANCKKDSKSF
AsTRPA1Ba 618 PEAALAMATHEERSGEVMALKSDKHPCVTLALIASMPRVFEAVQDNCITKANCKKDSKSF
AaTRPA1Ba 618 PEAALAMATHEERSAEVMALKSDKHPCVTLALIASMPRVFEAVQDNCISKANCKKDSKSF
AaTRPA1Bb 618 PEAALAMATHEERSAEVMALKSDKHPCVTLALIASMPRVFEAVQDNCISKANCKKDSKSF
* *

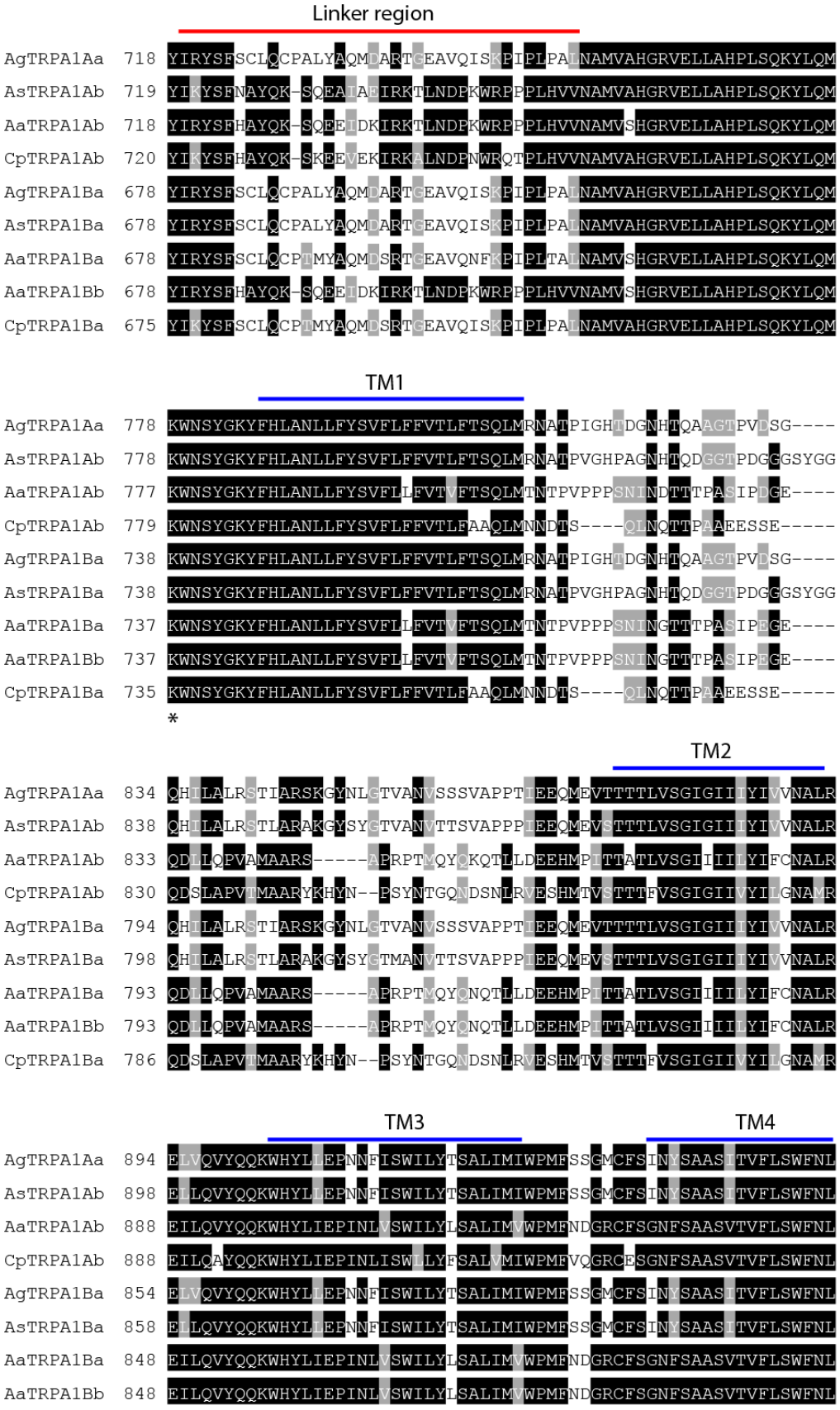
Linker region
TM1
TM2
TM3
TM4
AgTRPA1Aa 718
AsTRPA1Ab 719
AaTRPA1Ab 718
CpTRPA1Ab 720
AgTRPA1Ba 678
AsTRPA1Ba 678
AaTRPA1Ba 678
AaTRPA1Bb 678
CpTRPA1Ba 675
AgTRPA1Aa 778
AsTRPA1Ab 778
AaTRPA1Ab 777
CpTRPA1Ab 779
AgTRPA1Ba 738
AsTRPA1Ba 738
AaTRPA1Ba 737
AaTRPA1Bb 737
CpTRPA1Ba 735
AgTRPA1Aa 834
AsTRPA1Ab 838
AaTRPA1Ab 833
CpTRPA1Ab 830
AgTRPA1Ba 794
AsTRPA1Ba 798
AaTRPA1Ba 793
AaTRPA1Bb 793
CpTRPA1Ba 786
AgTRPA1Aa 894
AsTRPA1Ab 898
AaTRPA1Ab 888
CpTRPA1Ab 888
AgTRPA1Ba 854
AsTRPA1Ba 858
AaTRPA1Ba 848
AaTRPA1Bb 848

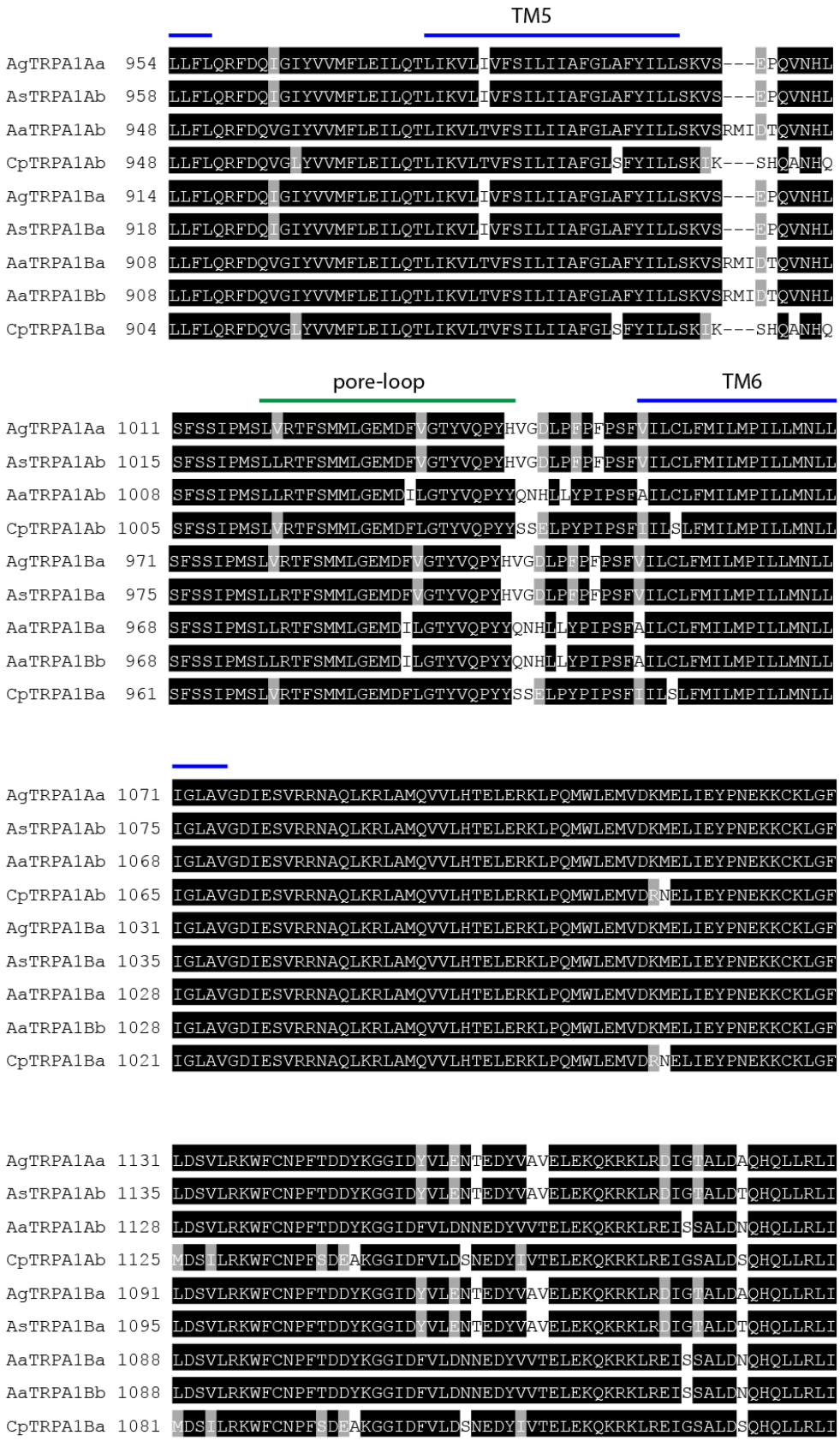
TM5
AgTRPA1Aa 954 LLFLQRFDQIGIYVVMFLEILQTLIKVLIVFSILIIAFGLAFYILLSKVS---EPQVNHL
AsTRPA1Ab 958 LLFLQRFDQIGIYVVMFLEILQTLIKVLIVFSILIIAFGLAFYILLSKVS---EPQVNHL
AaTRPA1Ab 948 LLFLQRFDQVGIYVVMFLEILQTLIKVLTVFSILIIAFGLAFYILLSKVSRMIDTQVNHL
CpTRPA1Ab 948 LLFLQRFDQVGIYVVMFLEILQTLIKVLTVFSILIIAFGLSFYILLSKIK---SHQANHQ
AgTRPA1Ba 914 LLFLQRFDQIGIYVVMFLEILQTLIKVLIVFSILIIAFGLAFYILLSKVS---EPQVNHL
AsTRPA1Ba 918 LLFLQRFDQIGIYVVMFLEILQTLIKVLIVFSILIIAFGLAFYILLSKVS---EPQVNHL
AaTRPA1Ba 908 LLFLQRFDQVGIYVVMFLEILQTLIKVLTVFSILIIAFGLAFYILLSKVSRMIDTQVNHL
AaTRPA1Bb 908 LLFLQRFDQVGIYVVMFLEILQTLIKVLTVFSILIIAFGLAFYILLSKVSRMIDTQVNHL
CpTRPA1Ba 904 LLFLQRFDQVGIYVVMFLEILQTLIKVLTVFSILIIAFGLSFYILLSKIK---SHQANHQ
pore-loop
TM6
AgTRPA1Aa 1011 SFSSIPMSLVRTFSMMLGEMDFVGTYVQPYHVGDLPFPFPSFVILCLFMILMPILLMNLL
AsTRPA1Ab 1015 SFSSIPMSLLRTFSMMLGEMDFVGTYVQPYHVGDLPFPFPSFVILCLFMILMPILLMNLL
AaTRPA1Ab 1008 SFSSIPMSLLRTFSMMLGEMDILGTYVQPYYQNHLLYPIPSFAILCLFMILMPILLMNLL
CpTRPA1Ab 1005 SFSSIPMSLVRTFSMMLGEMDFLGTYVQPYYSSELPYPIPSFIILSLFMILMPILLMNLL
AgTRPA1Ba 971 SFSSIPMSLVRTFSMMLGEMDFVGTYVQPYHVGDLPFPFPSFVILCLFMILMPILLMNLL
AsTRPA1Ba 975 SFSSIPMSLLRTFSMMLGEMDFVGTYVQPYHVGDLPFPFPSFVILCLFMILMPILLMNLL
AaTRPA1Ba 968 SFSSIPMSLLRTFSMMLGEMDILGTYVQPYYQNHLLYPIPSFAILCLFMILMPILLMNLL
AaTRPA1Bb 968 SFSSIPMSLLRTFSMMLGEMDILGTYVQPYYQNHLLYPIPSFAILCLFMILMPILLMNLL
CpTRPA1Ba 961 SFSSIPMSLVRTFSMMLGEMDFLGTYVQPYYSSELPYPIPSFIILSLFMILMPILLMNLL
AgTRPA1Aa 1071 IGLAVGDIESVRRNAQLKRLAMQVVLHTELERKLPQMWLEMVDKMELIEYPNEKKCKLGF
AsTRPA1Ab 1075 IGLAVGDIESVRRNAQLKRLAMQVVLHTELERKLPQMWLEMVDKMELIEYPNEKKCKLGF
AaTRPA1Ab 1068 IGLAVGDIESVRRNAQLKRLAMQVVLHTELERKLPQMWLEMVDKMELIEYPNEKKCKLGF
CpTRPA1Ab 1065 IGLAVGDIESVRRNAQLKRLAMQVVLHTELERKLPQMWLEMVDRNELIEYPNEKKCKLGF
AgTRPA1Ba 1031 IGLAVGDIESVRRNAQLKRLAMQVVLHTELERKLPQMWLEMVDKMELIEYPNEKKCKLGF
AsTRPA1Ba 1035 IGLAVGDIESVRRNAQLKRLAMQVVLHTELERKLPQMWLEMVDKMELIEYPNEKKCKLGF
AaTRPA1Ba 1028 IGLAVGDIESVRRNAQLKRLAMQVVLHTELERKLPQMWLEMVDKMELIEYPNEKKCKLGF
AaTRPA1Bb 1028 IGLAVGDIESVRRNAQLKRLAMQVVLHTELERKLPQMWLEMVDKMELIEYPNEKKCKLGF
CpTRPA1Ba 1021 IGLAVGDIESVRRNAQLKRLAMQVVLHTELERKLPQMWLEMVDRNELIEYPNEKKCKLGF
AgTRPA1Aa 1131 LDSVLRKWFCNPFTDDYKGGIDYVLENTEDYVAVELEKQKRKLRDIGTALDAQHQLLRLI
AsTRPA1Ab 1135 LDSVLRKWFCNPFTDDYKGGIDYVLENTEDYVAVELEKQKRKLRDIGTALDTQHQLLRLI
AaTRPA1Ab 1128 LDSVLRKWFCNPFTDDYKGGIDFVLDNNEDYVVTELEKQKRKLREISSALDNQHQLLRLI
CpTRPA1Ab 1125 MDSILRKWFCNPFSDDAKGGIDFVLDSNEDYIVTELEKQKRKLREIGSALDSQHQLLRLI
AgTRPA1Ba 1091 LDSVLRKWFCNPFTDDYKGGIDYVLENTEDYVAVELEKQKRKLRDIGTALDAQHQLLRLI
AsTRPA1Ba 1095 LDSVLRKWFCNPFTDDYKGGIDYVLENTEDYVAVELEKQKRKLRDIGTALDTQHQLLRLI
AaTRPA1Ba 1088 LDSVLRKWFCNPFTDDYKGGIDFVLDNNEDYVVTELEKQKRKLREISSALDNQHQLLRLI
AaTRPA1Bb 1088 LDSVLRKWFCNPFTDDYKGGIDFVLDNNEDYVVTELEKQKRKLREISSALDNQHQLLRLI
CpTRPA1Ba 1081 MDSILRKWFCNPFSDDAKGGIDFVLDSNEDYIVTELEKQKRKLREIGSALDSQHQLLRLI

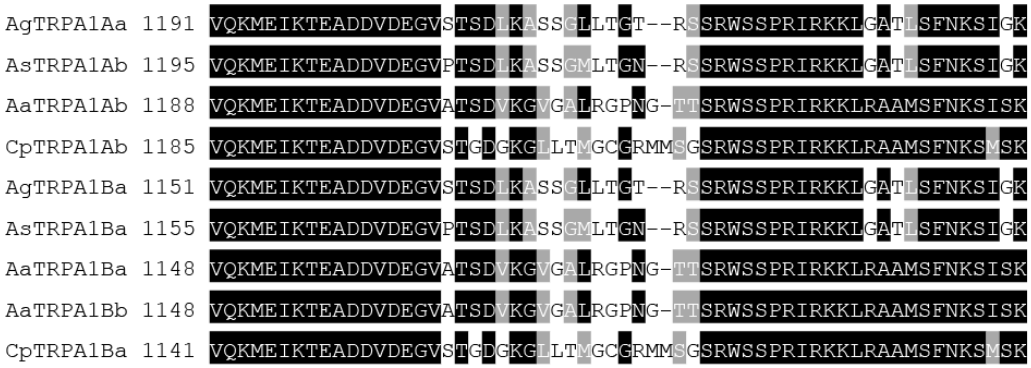

AgTRPA1Aa 1249 *

AsTRPA1Ab 1253 *

AaTRPA1Ab 1247 *

CpTRPA1Ab 1245 *

AgTRPA1Ba 1209 *

AsTRPA1Ba 1213 *

AaTRPA1Ba 1207 *

AaTRPA1Bb 1207 *

b

% amino acid identity

	AgTRPA1Aa	AgTRPA1Ba	AsTRPA1Ab	AsTRPA1Ba	AaTRPA1Ab	AaTRPA1Ba	AaTRPA1Bb	CpTRPA1Ab	CpTRPA1Ba
AgTRPA1Aa	100								
AgTRPA1Ba	99	100							
AsTRPA1Ab	94	90	100						
AsTRPA1Ba	92	97	97	100					
AaTRPA1Ab	82	80	84	79	100				
AaTRPA1Ba	79	84	82	85	97	100			
AaTRPA1Bb	79	83	82	83	99	98	100		
CpTRPA1Ab	79	78	81	77	84	81	81	100	
CpTRPA1Ba	80	83	82	83	79	86	84	97	100

Appendix 1. Protein sequence alignment of AgTRPA1Aa, AsTRPA1Ab, AaTRPA1Ab, CpTRPA1Ab, AgTRPA1Ba, AsTRPA1Ba, AaTRPA1Ba, AaTRPA1Bb and CpTRPA1Ba.

(a) Ankyrin repeats are labeled with black or grey bars, linker region is labeled with a red bar, transmembrane domains are labeled with blue bars, pore loop is labeled with a green bar. Asterisks note the reported conserved residues for electrophile detection. (b) Amino acid identity of the above TRPA1 protein.

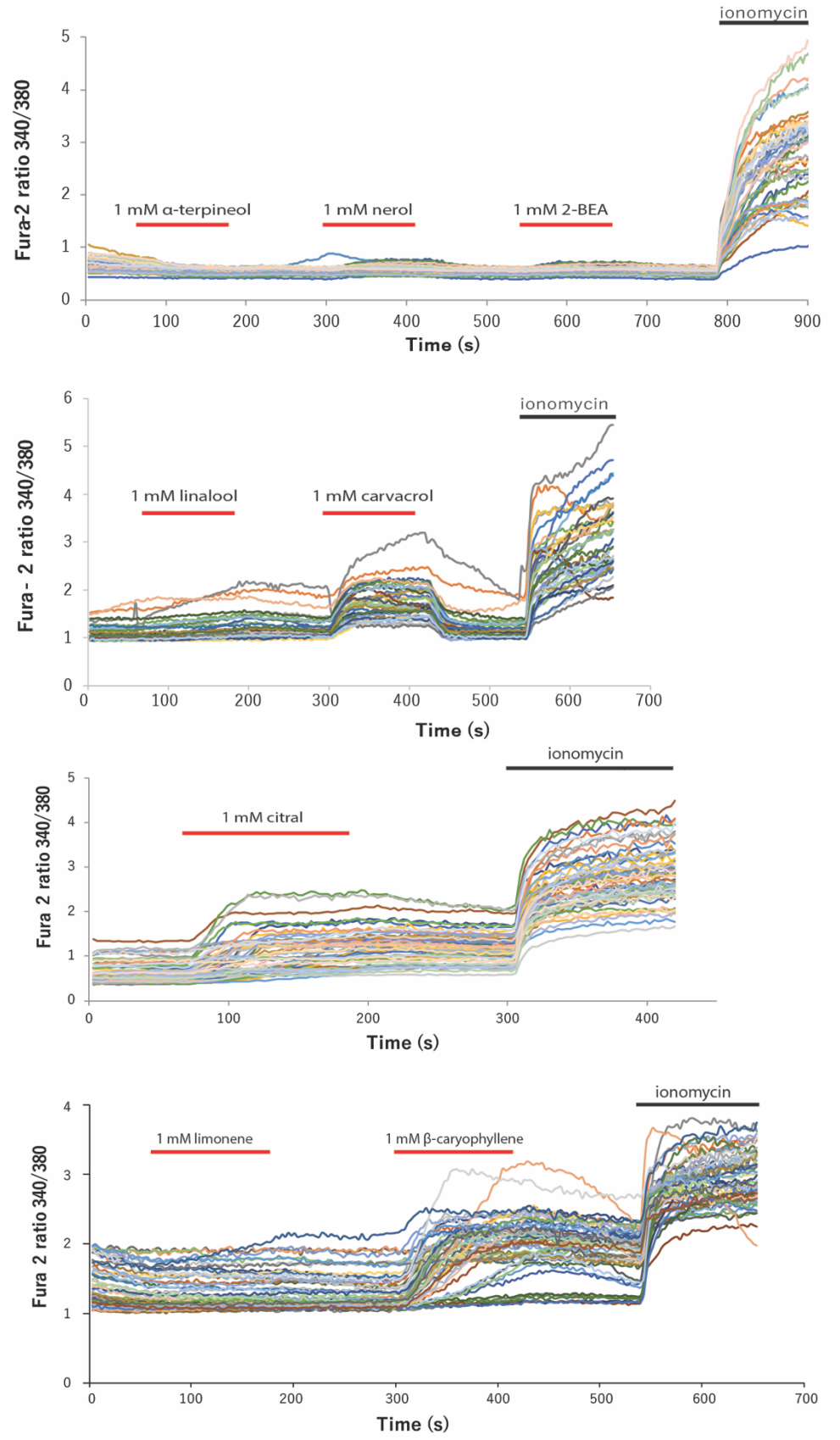
ionomycin
Fura-2 ratio 340/380
1 mM α-terpineol
1 mM nerol
1 mM 2-BEA
Time (s)
ionomycin
Fura - 2 ratio 340/380
1 mM linalool
1 mM carvacrol
Time (s)
ionomycin
Fura 2 ratio 340/380
1 mM citral
Time (s)
ionomycin
Fura 2 ratio 340/380
1 mM limonene
1 mM β-caryophyllene
Time (s)

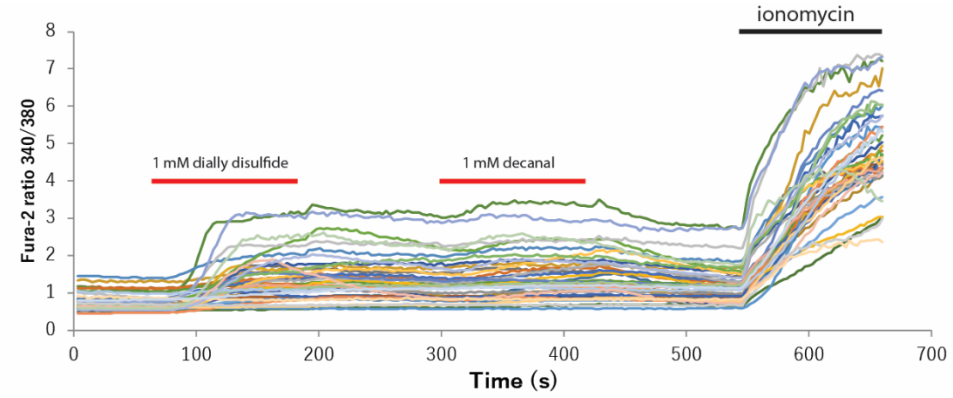
ionomycin
1 mM dially disulfide
1 mM decanal
Fura-2 ratio 340/380
Time (s)

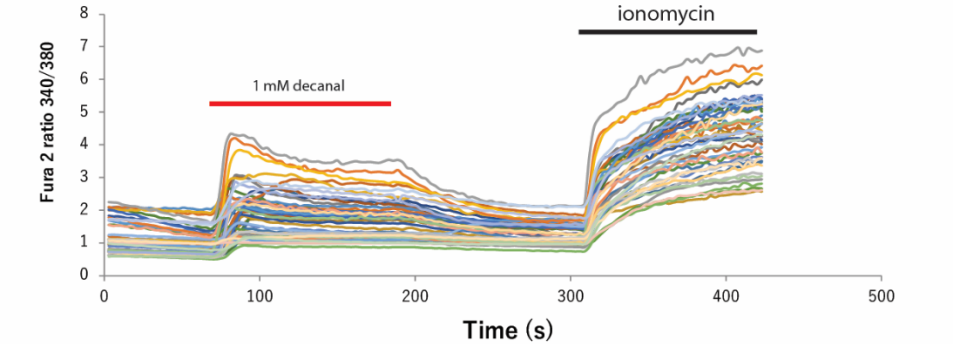
ionomycin
1 mM decanal
Fura 2 ratio 340/380
Time (s)

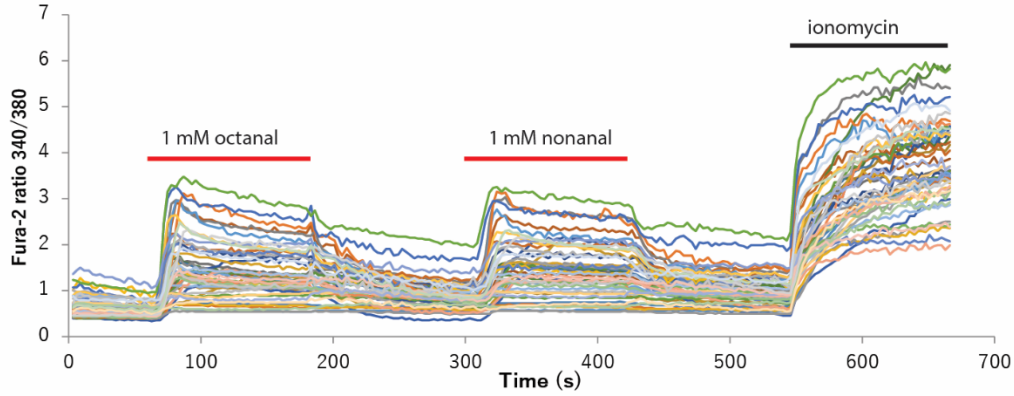
ionomycin
1 mM octanal
1 mM nonanal
Fura-2 ratio 340/380
Time (s)

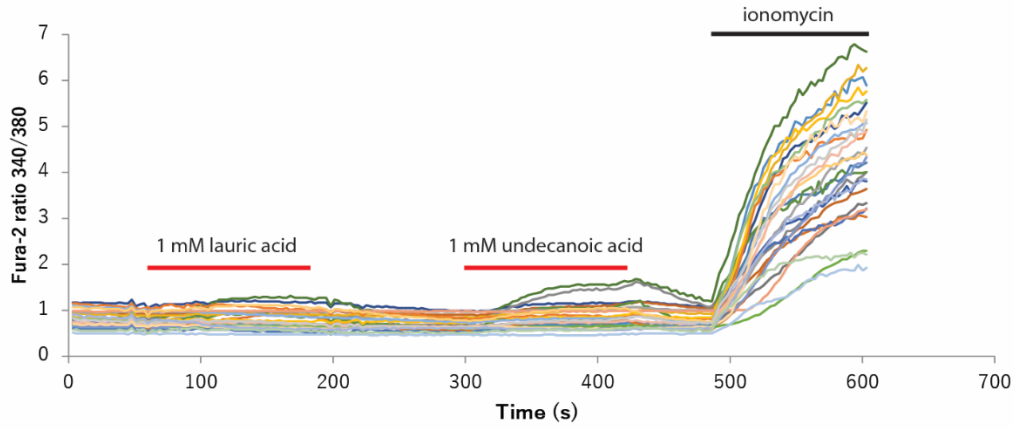
ionomycin
1 mM lauric acid
1 mM undecanoic acid
Fura-2 ratio 340/380
Time (s)

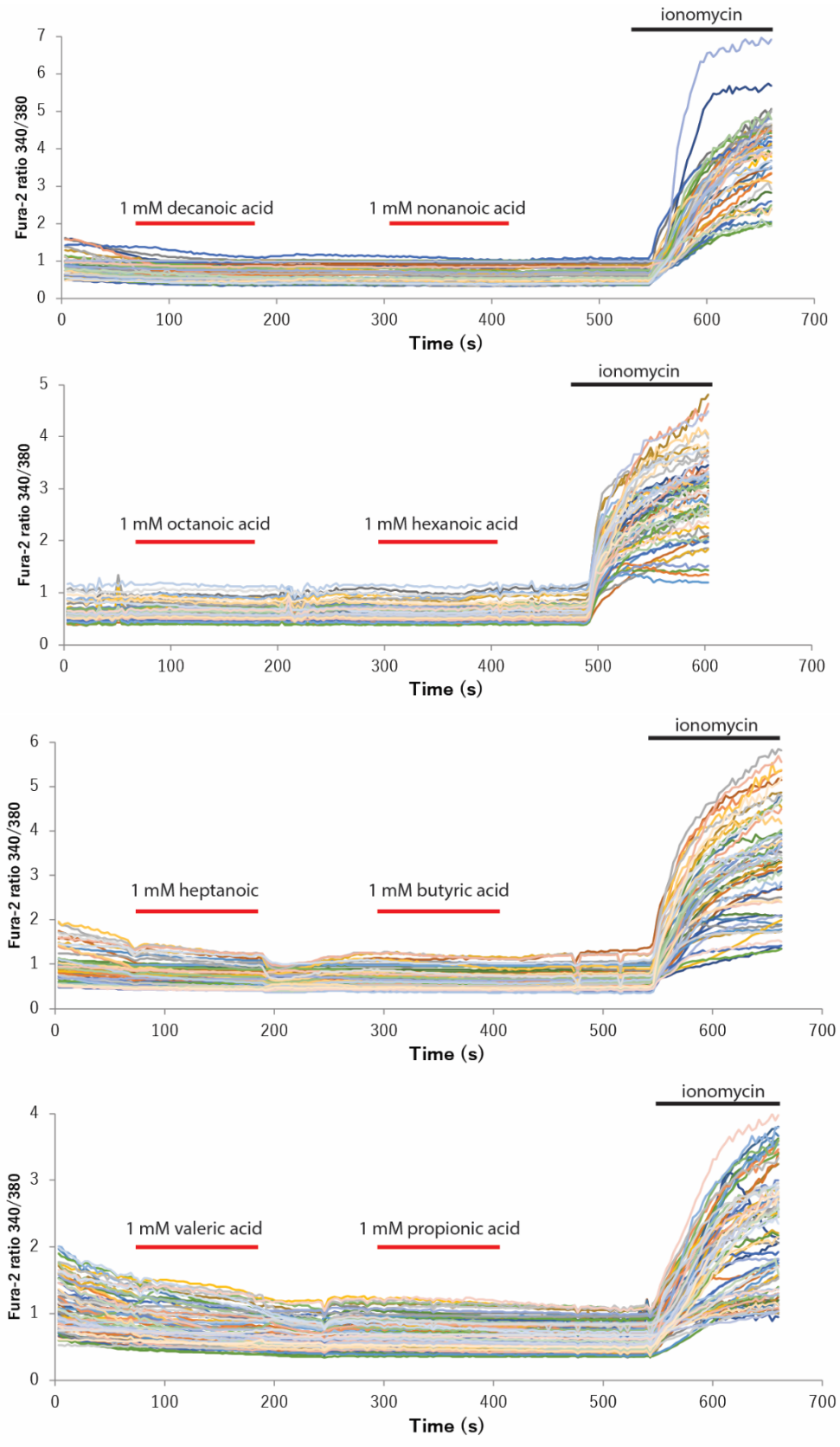
ionomycin
1 mM decanoic acid
1 mM nonanoic acid
Fura-2 ratio 340/380
Time (s)
ionomycin
1 mM octanoic acid
1 mM hexanoic acid
Fura-2 ratio 340/380
Time (s)
ionomycin
1 mM heptanoic
1 mM butyric acid
Fura-2 ratio 340/380
Time (s)
ionomycin
1 mM valeric acid
1 mM propionic acid
Fura-2 ratio 340/380
Time (s)

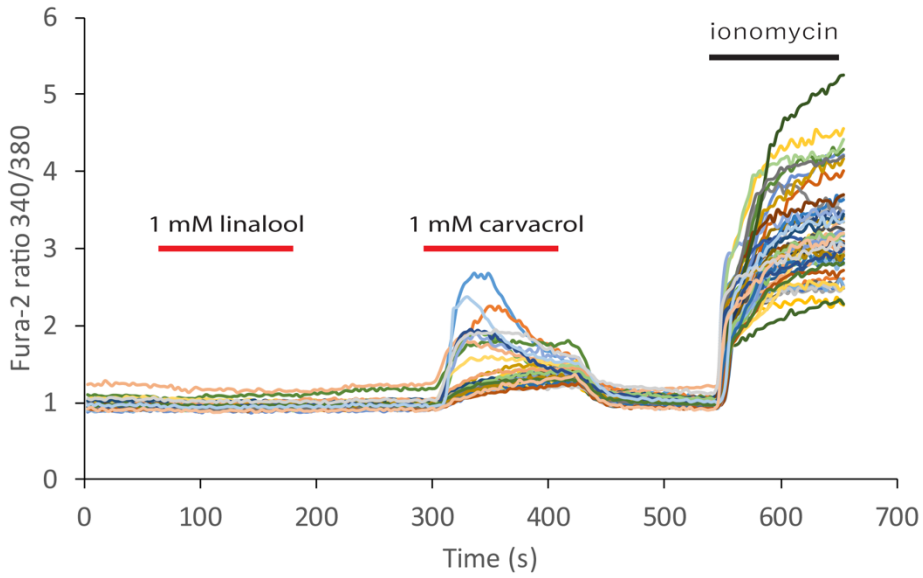

Appendix 2. Representative calcium imaging traces for testing the effects of the chemicals (section 2.7) on AgTRPA1Ba(S). Octanal, nonanal and decanal evoked great increase in intracellular calcium concentrations, and citral also evoked slight increase in intracellular calcium concentrations in cells expressing AgTRPA1Ba(S). Two other pungent compounds, β-caryophyllene and diallyl disulfide, could evoke increase in intracellular calcium concentrations as well.